Article

Comparative transcriptomics of multi-stress responses in *Pachycladon cheesemanii* and *Arabidopsis thaliana*

Yanni Dong [1], Saurabh Gupta [2,†], Jason J. Wargent [3], Joanna Putterill [4], Richard Macknight [5], Tsanko Gechev [6,7], Bernd Mueller-Roeber [2,6,8] and Paul Dijkwel [1,*]

[1] School of Natural Sciences, Massey University, Tennent Drive, Palmerston North 4474, New Zealand
[2] Department Molecular Biology, Institute of Biochemistry and Biology, University of Potsdam, Karl-Liebknecht-Straße 24-25, Haus 20, 14476 Potsdam, Germany
[3] School of Agriculture & Environment, Massey University, Palmerston North 4442, New Zealand
[4] School of Biological Sciences, University of Auckland, Auckland, New Zealand
[5] Biochemistry Department, School of Biomedical Sciences, University of Otago, Dunedin, New Zealand
[6] Center of Plant Systems Biology and Biotechnology (CPSBB), 139 Ruski Blvd., Plovdiv 4000, Bulgaria
[7] Department of Plant Physiology and Plant Molecular Biology, University of Plovdiv, 24 Tsar Assen str., Plovdiv 4000, Bulgaria
[8] Max Planck Institute of Molecular Plant Physiology, Am Mühlenberg 1, 14476 Potsdam, Germany
* Correspondence: p.dijkwel@massey.ac.nz
† **Present address:** Curtin Medical School, Curtin University, 410 Koorliny Way, Bentley, WA 6102, Australia

Abstract: The environment is seldom optimal for plant growth and changes in abiotic and biotic signals, including temperature, water availability, radiation and pests, induce plant responses to optimise survival. The New Zealand native plant species and close relative to *Arabidopsis thaliana*, *Pachycladon cheesemanii* grows under environmental conditions that are unsustainable for many plant species. Here we compare the responses of both plant species to different stressors (low temperature, salt and UV-B radiation) to help understand how *P. cheesemanii* can grow in such harsh environments. The stress transcriptomes were then determined and comparative transcriptome and network analyses discovered similar and unique responses within species between different stresses, and between the two plant species. A number of widely studied plant stress processes were highly conserved in *A. thaliana* and *P. cheesemanii*. However, in response to cold stress, Gene Ontology terms related to glycosinolate metabolism were only enriched in *P. cheesemanii*. Salt stress was associated with alteration of the cuticle and proline biosynthesis in *A. thaliana* and *P. cheesemanii*, respectively. Anthocyanin production may be a strategy to cope with UV-B radiation stress in *P. cheesemanii* only. These results allowed us to construct broad stress response pathways in *A. thaliana* and *P. cheesemanii* and identify possible novel plant strategies that help mitigate environmental stress.

Keywords: multi-stress responses; Arabidopsis; comparative transcriptomics; Pachycladon; cross-species comparison; network analysis

1. Introduction

Plants survive under various environmental stresses by responding at physiological, biochemical, cellular and molecular levels [1–4]. Plants adapt to their environment throughout their lifetime. In addition, over evolutionary time, plants evolve to mount effective responses to environmental cues such as UV-B radiation, drought, high or low temperature and salinity [5–7].

The ability to estimate the expression of thousands of genes of a single sample has allowed the identification of complex stress-induced expression networks and considerable overlap between distinct stresses, and interactions within stress networks were found: A cDNA microarray analysis of drought, cold and high salinity-treated rice plants demonstrated a wide range of cross talk involving 15 common stress-induced genes [8]. Also, 232 clones were common among responses to

 doi:10.20944/preprints202305.1588.v1

cold, heat and salt stresses in potato plants, as revealed by analysis of cDNA microarray data [9]. More recently, a meta-analysis of publicly available rice RNA-seq data revealed that photosynthesis is down-regulated in response to both abiotic and biotic stress, and significant expression changes were found in genes involved in abscisic acid (ABA), jasmonic acid (JA) and salicylic acid (SA) signalling pathways [10]. In addition, this study found that a number of genes were uniquely induced by abiotic or biotic stress, but this was not further analysed. In *Arabidopsis thaliana*, 390 microarray samples (from 29 microarray studies) were analysed for comparing drought and cold stress responses. This identified 2890 differentially expressed genes in both stress responses with similar expression patterns. Moreover, 21 drought and 16 highly inter-correlated cold gene modules were identified with four consensus gene modules, but few stress-specific genes were mentioned [11]. Osmotic stress is the primary signal which is caused by both drought and salt stress, and salt stress has ionic effects on cells as well [12]. Also, both stresses induce oxidative stress and damage to the membrane system [13]. Thus, drought and salt stresses have unique and overlapping responses [14]. The comparative transcriptome analysis of *Iris lactea* var. *chinensis* under drought and salt stress showed that, against the untreated control, 3897 differentially expressed genes had the same expression pattern. Nevertheless, GO enrichment analysis revealed that while the responses were largely the same, a number of unique GO terms were enriched only in the drought or salt stress response, suggesting that this plant species can distinguish between the two related stresses [15]. Thus, high-throughput expression profiling can help identify comprehensive crosstalk among multiple stress responses. Nevertheless, few studies have compared transcriptome differences between multiple stress responses of related plant species. As part of a gene co-expression analysis of four cotton species in response to cold and salt stress, 29 co-expression modules displayed significant correlations with at least one of seven sample conditions which included the four genomes, cold stress, salt stress, and cold and salt stress. However, four major modules were most strongly correlated with each of the four genomes, suggesting these highly co-expressed genes were species-specific. This study evidenced the presence of evolutionary divergence and the potential shared network of cold and salt response among four related species [16].

In contrast to drought, temperature and biotic stress, plant UV-B radiation responses have been studied relatively independently from other stresses in *Arabidopsis* and other plant species [17–20]. Nevertheless, high-throughput analyses have resulted in a deeper understanding of plant UV-B radiation response pathways. After exposure of maize (*Zea mays*) plants to 9 kJ m^{-2} d^{-1} UV-B radiation, a number of transcripts were upregulated or downregulated significantly in at least one organ [21]. A microarray analysis of the gene expression responses of grape (*Vitis vinifera* L.) leaves to UV-B radiation (4.75 kJ m^{-2} d^{-1}) revealed that plant responses could be categorised as general protective responses (synthesis of UV-B absorbing compounds), antioxidant defence, pathogen defence and abiotic stress responses [22]. RNA-seq analysis was performed on *Lycium ruthenicum* with and without UV-B induction, involving 1,913 upregulated and 536 downregulated genes that included antioxidant-related genes and genes involved in secondary metabolite synthesis and defence responses [23]. However, there are few reports describing the interaction between UV-B and other stress responses. An exception is in the frame of the AtGenExpress project, where Affymetrix ATH1 microarray analyses of multiple stress regulatory networks consisting of heat, cold, drought, salt, high osmolarity, UV-B radiation and wounding were compared. The results suggested the existence of a set of core genes in *Arabidopsis* that initially respond to all these environmental stresses [24].

Here, we studied *Pachycladon cheesemanii*, a tetraploid genus of Brassicaceae and native to New Zealand and compared it to its relative, *Arabidopsis thaliana*. *P. cheesemanii* has a wide latitudinal and altitudinal range, from near sea level to 1600 m where it is subject to relatively high levels of UV-B radiation and a mean winter temperature of 2–5 °C [7,25]. Also, this species grows on diverse rock substrate (greywacke, haast schist, and basaltic and andesitic volcanic rocks) which could impact growth via soil nutrient availability [25,26]. Thus, these diverse environmental conditions likely have caused the development of adaptive characteristics in this species, including UV-B tolerance [7]. In comparison, *Arabidopsis thaliana* ecotypes distribute through Western Eurasia with wide temperature ranges of -20-17.5 °C and precipitation (11.5-190 mm) over the year [27]. Nevertheless, the widely

 doi:10.20944/preprints202305.1588.v1

used laboratory accession, Col-0, was collected from Columbia, United States of America, with a daily temperature 15-16/21-22 °C and a monthly precipitation of 30-70 mm (ABRC, Arabidopsis Biological Resource Center). Although the two plant species are close relatives, *P. cheesemanii* experienced a genome duplication event, a relatively short 1.61 million years ago, where one of the *P. cheesemanii* sub-genomes was proposed to have the same origin as *A. thaliana*'s genome [28]. The different living niches most likely have caused the development of species-specific characteristics over evolutionary time, while the genome duplication event may have provided the means for genes to evolve new functions in *P. cheesemanii*. Thus, comparing how *P. cheesemanii* and *A. thaliana* respond to different stresses could help deepen our understanding of how the environment shapes plant evolution and adaptation.

Here, we present an interaction model that describes the correlating gene networks responding to cold, salt and UV-B radiation stress in two related plant species, *A. thaliana* and *P. cheesemanii*. The study confirmed that conserved pathways exist, but also considerable species-specific response pathways were identified, possibly driven by evolutionary selective processes.

2. Results

2.1. Abiotic stress transcriptomes of A. thaliana and P. cheesemanii

Changes in gene expression caused by different abiotic stresses were investigated by analysing the transcriptomes of stressed and unstressed *A. thaliana* and *P. cheesemanii* plants using an RNA-seq approach. Six-week-old *A. thaliana* and nine-week-old *P. cheesemanii* plants were treated at 4°C, 250 mM NaCl or 5.2 µmol m^{-2} s^{-1} UV-B radiation. This UV-B radiation level was shown to cause different responses of *A. thaliana* and *P. cheesemanii* [7]. Treated and control plants were collected after 5 hours of treatment to detect early transcriptional changes. Total RNA was extracted from treated and untreated leaves to result in 12 samples for each of the species; 3 biological replicates for each of the stresses and the control. The 24 RNA samples were used for RNA-seq as described in Materials and methods.

The *A. thaliana* transcriptome is available online (GenBank CP002684–CP002688) and contains 27,656 genes. We generated a *P. cheesemanii* transcriptome by RNA-seq as follows: The 12 *P. cheesemanii* Illumina libraries of 2 × 150-bp paired-end (PE) reads were sequenced for a total of 122.11 GB of sequence from 437,025,992 clean reads (**Table S1**). A *de novo* transcriptome assembly of 67,905 transcripts was generated as described in Materials and methods (**File S1**). Transcript length distribution analysis revealed that 73.98% of transcripts were between 200 and 2,000 bp, with 1% being longer than 5,000 bp (**Figure S1a**). The Benchmarking Universal Single-Copy Ortholog (BUSCO) assessment results showed that 94.7% of BUSCOs could be found in the set as single (48.7%) or duplicate (46.0%) copy. Fragmented and missing BUSCOs were rare, i.e., 2.7% and 2.6%, respectively (**Figure S1b**). These results demonstrated the high-quality integrity of the *P. cheesemanii* transcript set and validated it for use in downstream analysis.

2.2. Differentially expressed gene number bias in the three stress responses of A. thaliana and P. cheesemanii

Using the transcriptomes of the two plant species, the RNA-seq data were used to discover genes significantly differentially expressed (DE) in response to cold, salt or UV-B treatment. We used edgeR with Trimmed Mean of M-values (TMM) normalization in all treatments [29]. **Table 1** shows that between ~800 and 4,000 genes were significantly DE in response to cold, salt or UV-B treatment, out of 27,656 *A. thaliana* and 67,905 *P. cheesemanii* genes. Salt stress induced the least number of DE genes in both plant species. A volcano plot analysis showed considerable DE gene number bias in both plant species (**Figure 1**) with salt stress showing ~4-fold more upregulated than downregulated genes. In *P. cheesemanii*, UV-B radiation (~4-fold) and cold (~2-fold) stress also caused a similar bias which was not found in *A. thaliana*.

Thus, while the number of DE genes in response to each stress was broadly similar in the two species, there was considerable DE gene expression bias.

Preprints (www.preprints.org) | NOT PEER-REVIEWED | Posted: 23 May 2023 doi:10.20944/preprints202305.1588.v1

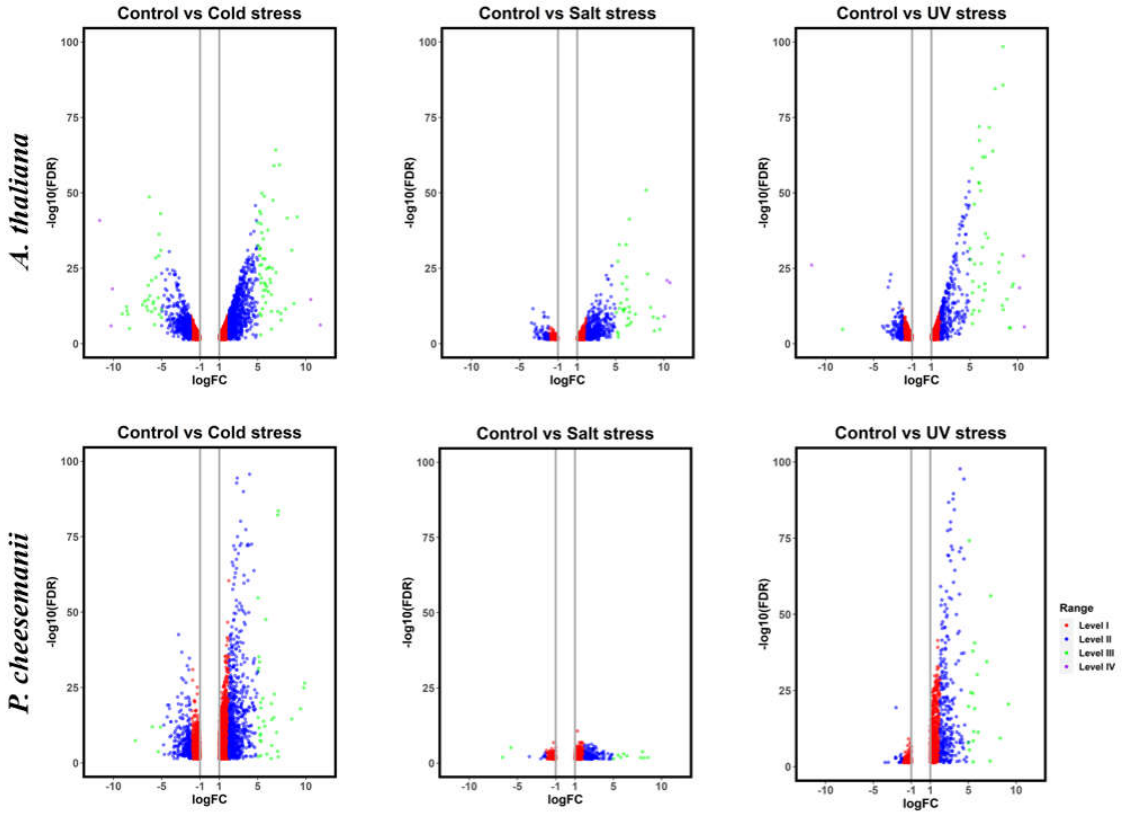

Figure 1. Differential gene expression of *P. cheesemanii* and *A. thaliana* caused by different stresses. Volcano plots showing fold change in abundance (logFC) against significance show DE genes in response to cold, salt, and UV-B radiation stress. FC: fold change; FDR: false discovery ratio. Upper row: *A. thaliana*; lower row: *P. cheesemanii*. The differentially expressed genes were grouped into 4 levels with different colours: Level I, orange; Level II, blue; Level III, green; Level IV, purple.

Table 1. Summary of differentially expressed genes in multiple stresses in *A. thaliana* and *P. cheesemanii*. To group genes based on their expression levels the following expression categories were defined: Level I, with 2≤|FC|<4; Level II, with 4≤|FC|<32; Level III, with 32≤|FC|<1024 and Level IV, with 1024≤|FC|. FC, fold change.

Species	Stress	Upregulated genes	Downregulated genes	Level I	%	Level II	%	Level III	%	Level IV	%	Total
	Cold	2,060	1,911	2,641	66.5	1,242	31.3	83	2.1	5	0.1	3,971
A. thaliana	Salt	869	185	596	56.5	423	40.1	32	3.0	3	0.3	1,054
	UV-B	1,181	1,033	1,763	79.6	404	18.2	43	1.9	4	0.2	2,214
	Cold	2,509	1,181	2,730	74.0	918	24.9	42	1.1	0	0	3,690
P. cheesemanii	Salt	620	186	635	78.8	160	19.9	11	1.4	0	0	806
	UV-B	1,005	237	937	75.5	284	22.9	20	1.6	0	0	1,242

2.3. Comparative analysis of stress-responsive gene sets

Next, we examined the relationship between stress responses by identifying responsive genes shared among stresses, as well as responsive genes unique to each stress within species. The responsive genes that were upregulated and downregulated were compared between stresses using a Venn diagram analysis as shown in **Figure 2**. As expected, upregulated transcripts due to one stress were more likely to be upregulated by another stress than downregulated, apart from one notable exception where in *P. cheesemanii* more salt-downregulated genes were upregulated than downregulated by cold stress. Furthermore, in both plant species, salt- and UV-B-radiation-upregulated genes showed considerable overlap with cold-upregulated genes, while UV-B-radiation-upregulated genes showed little overlap with salt-upregulated ones. In general, while different stress

Preprints (www.preprints.org) | NOT PEER-REVIEWED | Posted: 23 May 2023 doi:10.20944/preprints202305.1588.v1

responses shared a number of responsive genes, the majority of responsive genes were unique to each stress response within species.

Nevertheless, DE genes were selected using strict cut-off parameters and genes that are strongly upregulated under one stress may still be upregulated by another stress, but not identified as a result of the parameters used. Therefore, we also compared the stress responses by means of overlapping GO terms associated with the DE genes. GO enrichment analysis was performed and the overrepresented terms for GO biological processes were compared among stresses using a Venn diagram (**Figure 3** and **File S2**). Overlap in GO terms was considerable between all stresses. Nevertheless, the UV-B radiation response in *A. thaliana* appeared more distinct from the others and that in *P. cheesemanii*, while the salt response included genes with comparatively less unique GO terms than those in the cold and UV-B radiation responses.

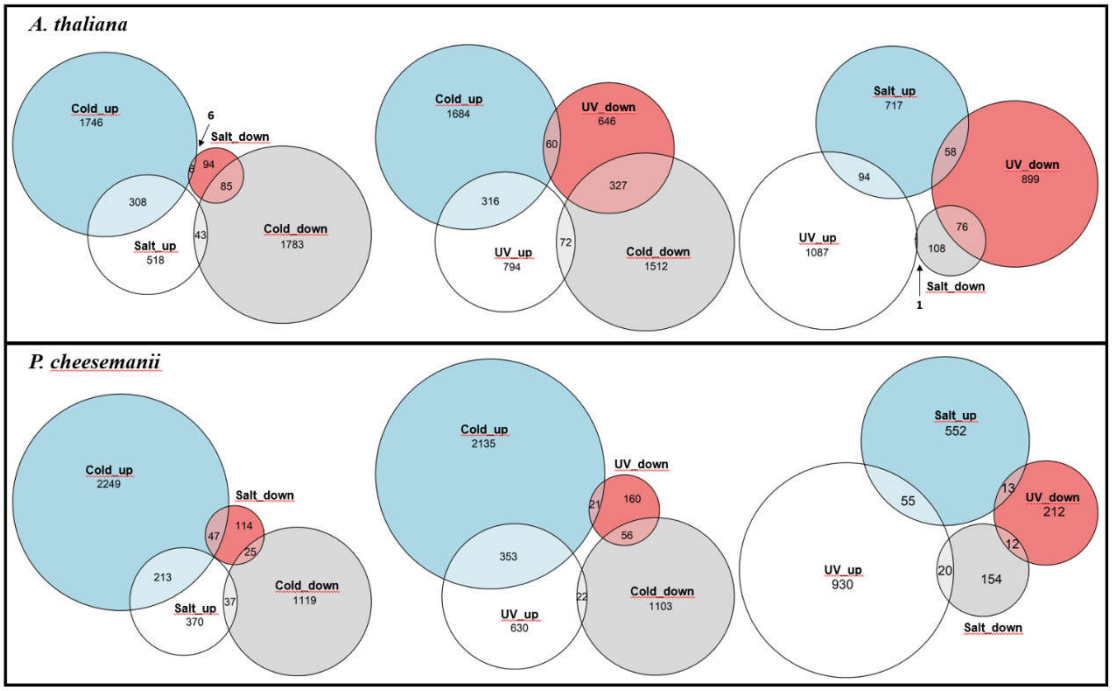

Figure 2. Venn diagrams of up- and down-regulated genes in response to stress in *A. thaliana* and *P. cheesemanii*. The diagrams show the number of up- and down-regulated genes and overlap in response to cold, salt, and UV-B radiation. Upper row: *A. thaliana*; lower row: *P. cheesemanii*.

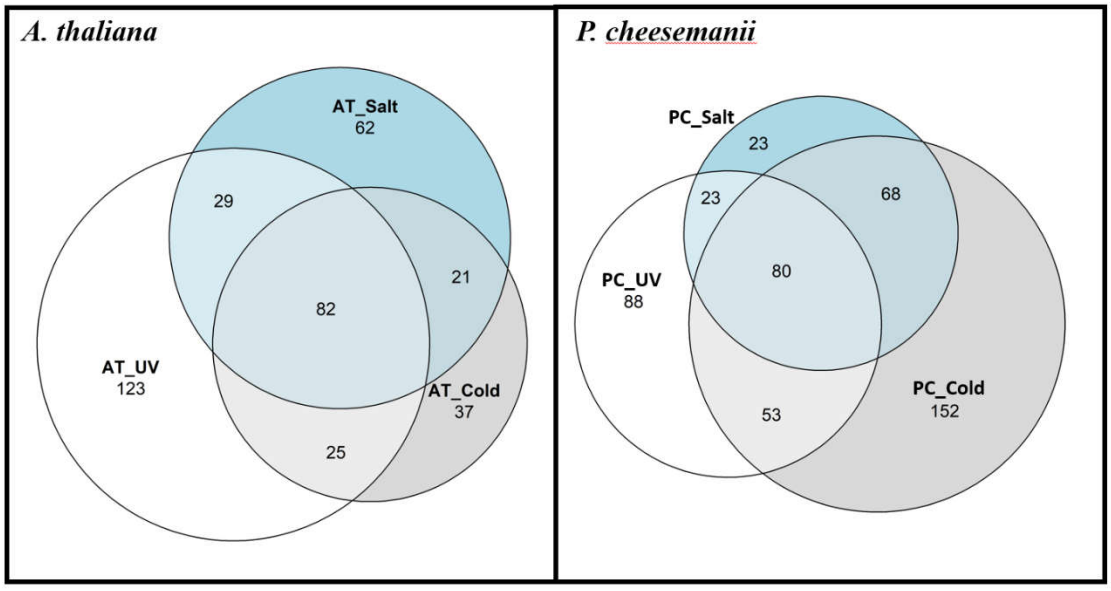

 doi:10.20944/preprints202305.1588.v1

Figure 3. Venn diagram of GO terms of biological processes between stresses in *A. thaliana* and *P. cheesemanii*. PC: *P. cheesemanii*; AT: *A. thaliana*; UV circles: the overrepresented GO terms in UV-B radiation response; Cold circles: the overrepresented GO terms in cold response; Salt circles: the overrepresented GO terms in salt response.

2.4. Network analysis identifies multiple stress-responsive crosstalks in A. thaliana and P. cheesemanii

To further discover crosstalk involving multiple stress responses, GO enrichment networks of multiple stress responses were generated from the stress-transcriptomes of *A. thaliana* and *P. cheesemanii*. GO terms were organised in a network where connections were created based on overlap between the gene sets using weighted correlation network analysis (WGCNA) and gene set enrichment analysis (GSEA), as described in Materials and methods. The network-layout groups related GO terms into network clusters, so that major overrepresented functional themes can be identified. **Figure 4** shows the *A. thaliana* network analysis of upregulated pathways. Salt and cold responses shared 'Response to stress and hormone stimulus', 'Response to hormone and ABA'; cold and UV-B stress responses shared 'Flavone and flavone biosynthesis' and 'Biological regulation'; salt and UV-B responses only shared 'Monosaccharide signalling: glucose and hexose'. Only a few network nodes within 'Response to UV' were shared among all three stress responses.

In the downregulation network, both cold and salt treatments included over-represented GO terms in 'DNA geometric change', while cold and UV-B stress downregulated GO terms in 'Immune response' and 'Response to wounding' (**Figure S2**).

Unlike the multi-stress network in *A. thaliana*, *P. cheesemanii* network showed few clusters (**Figure 5**). The main cluster that included all three stress responses was 'Response to stress', including some typical stress-related biological processes like response to stress hormones and anthocyanin biosynthesis.

Overall, there was a wide overlap between stress responses in *A. thaliana* in both upregulation and downregulation, while *P. cheesemanii* differed in having only one main cluster identified.

Preprints (www.preprints.org) | NOT PEER-REVIEWED | Posted: 23 May 2023 doi:10.20944/preprints202305.1588.v1

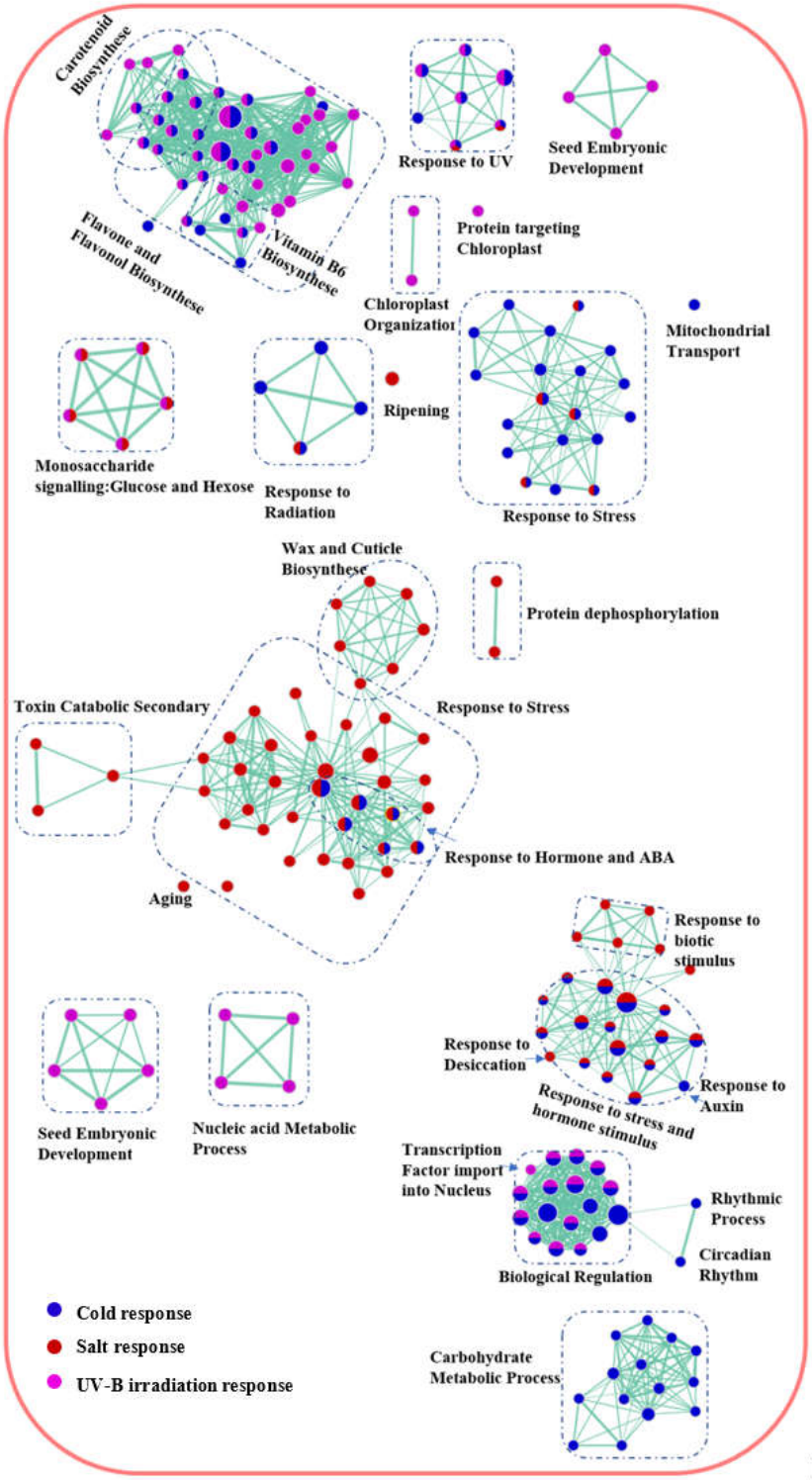

Figure 4. Network analysis of upregulated biological process of *A. thaliana* multiple stress-responsive transcriptomes. Purple, red and blue circles: overrepresented GO terms in response to UV-B radiation, salt and cold stress, respectively. Box with dashed line: cluster of the overrepresented GO terms involved in similar biological processes.

Preprints (www.preprints.org) | NOT PEER-REVIEWED | Posted: 23 May 2023 doi:10.20944/preprints202305.1588.v1

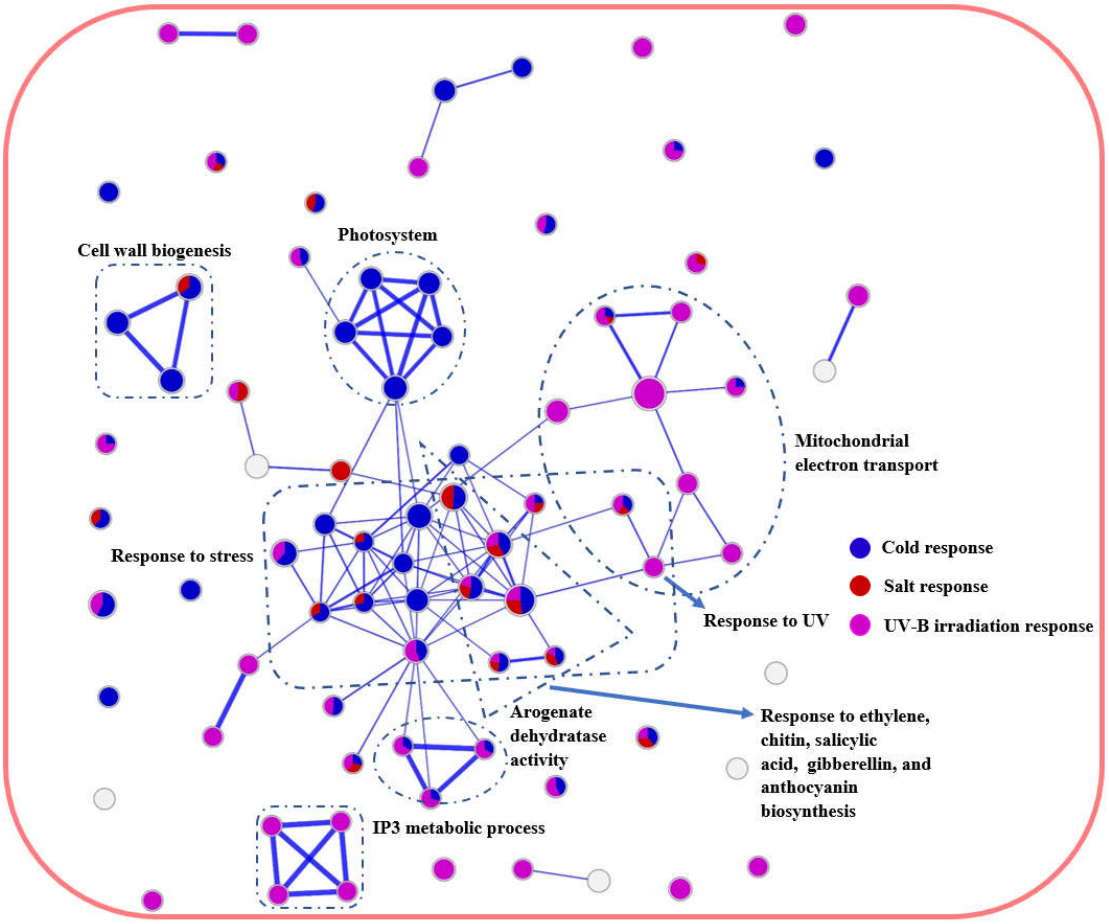

Figure 5. Network analysis of biological process of *P. cheesemanii* multiple stress-responsive transcriptomes. Purple, red and blue circles: overrepresented GO terms in response to UV-B radiation, salt and cold stress, respectively. Box with dashed line: cluster of the overrepresented GO terms involved in similar biological processes.

2.5. Identification of biological processes shared between A. thaliana and P. cheesemanii stress responses

To pinpoint the shared biological process between the two species in responding to each stress, overrepresented terms for GO biological processes in each stress were compared between the two species. **Figure 6** shows the results of this analysis using a Venn diagram and shows that salt and UV-B stress causes overrepresentation of about the same number of unique and shared GO terms in *A. thaliana* and *P. cheesemanii*. In contrast, cold stress causes overrepresentation of many more GO terms in *P. cheesemanii* than in *A. thaliana*, and those of *P. cheesemanii* included most of those of *A. thaliana*.

Next, we aimed to obtain an overall structure of responses common to both species. In each stress response, the overrepresented terms for GO biological processes (FDR < 0.05) of the two species were selected for further comparison. In response to cold, 74 overrepresented GO terms, with a similar percentage of induced genes, were shared by *A. thaliana* and *P. cheesemanii*, and the overrepresented GO terms were clustered into 13 groups (**Figures 7a** and **S2**). Then, we used REVIGO to summarise and visualise the GO terms [30] as described in the Materials and methods section. **Figure 7a** shows the resulting scatterplot of the common cold response, where the GO terms are placed in a semantic space, and clusters indicate semantic similarity among the terms within that cluster. Representative GO terms are then shown based on their dispensability values (<0.15) and visual inspection. The results suggest that in both *A. thaliana* and *P. cheesemanii* a wound-like response is initiated and that circadian rhythm (in plants only circadian rhythm is relevant within rhythmic process) as well as secondary metabolism, including those of flavonoids, trehalose, phenylpropanoid and oxylipin, is important during the early cold response. Most of the representative GO terms had

 doi:10.20944/preprints202305.1588.v1

similar percentages of upregulated and downregulated genes in *A. thaliana* and *P. cheesemanii* except flavonoid metabolism and regulation of response to stimulus (**Figure S3**).

The common salt response included 26 GO terms, and the REVIGO analysis indicated relatively generic GO terms, including the cluster 'Response to stimulus', 'Regulation of abscisic acid-activated signalling pathway' and 'Regulation of response to stimulus' (**Figure 7b**). The results suggest that the salt response may either be a generic response, or both species may respond to this stress in unique ways (**Figure S4**).

The common UV-B radiation response included 65 overrepresented GO terms and REVIGO indicated clusters summarised by 'Vitamin, L-phenylalanine, chorismite, L-ascorbic acid, and aromatic amino acid metabolic process' and response to stimulus. Other representative terms include those associated with secondary metabolism and pigments in particular and photosynthesis and light harvesting. The representative GO terms of these clusters also had similar rates of upregulated and downregulated genes in both species except cellular amine metabolic process, response to stimulus, and secondary metabolic process (**Figure S5**).

Overall, the analysis suggests that both species commonly use generic processes, including secondary metabolism as an early response to stress.

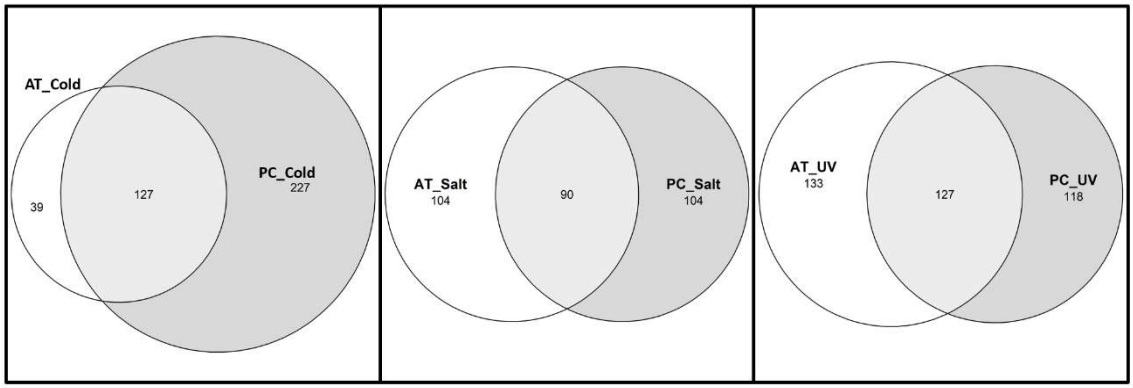

Figure 6. Venn diagrams of overrepresented GO terms of *A. thaliana* and *P. cheesemanii* in response to different stresses. Species-specific and overlapping number of overrepresented GO terms in response to cold, salt and UV-B radiation stress. PC: *P. cheesemanii*; AT: *A. thaliana*; UV circles: the overrepresented GO terms in UV-B radiation (UV) response.

Preprints (www.preprints.org) | NOT PEER-REVIEWED | Posted: 23 May 2023 doi:10.20944/preprints202305.1588.v1

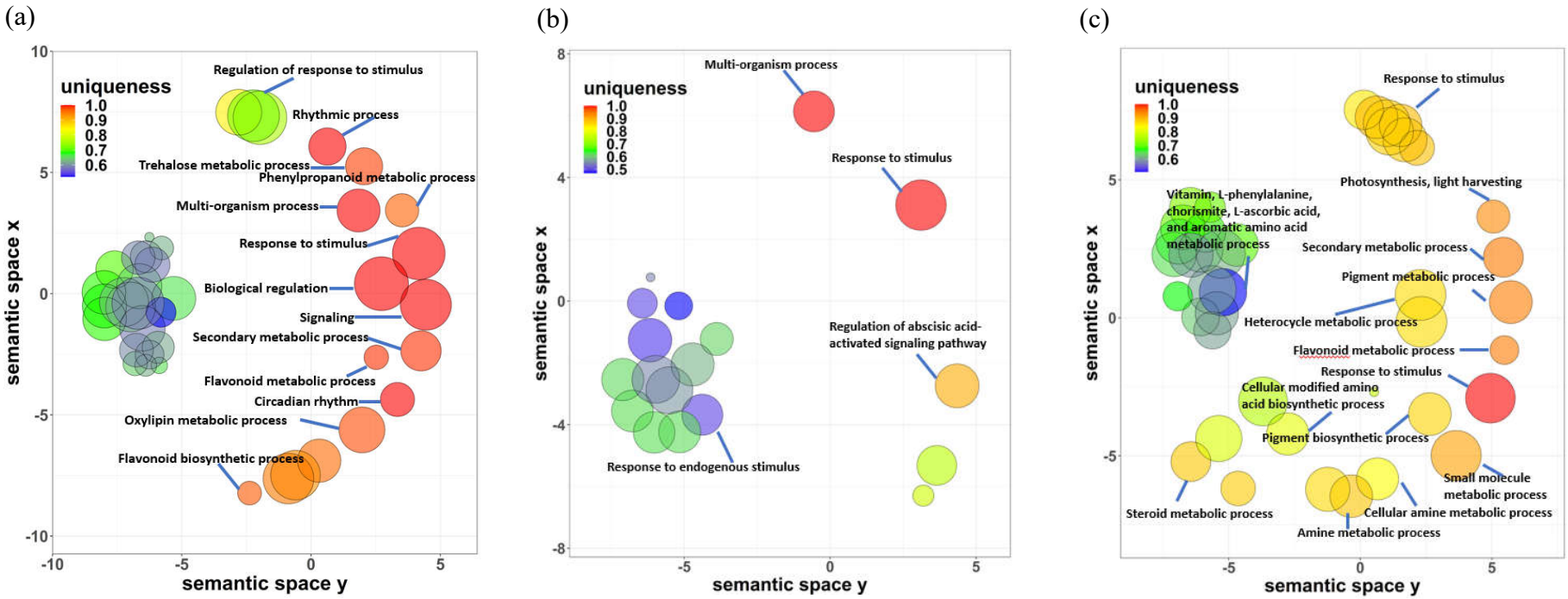

Figure 7. common GO biological process of *A. thaliana* and *P. cheesemanii* in response to cold, salt and UV-B radiation stress. Clustering of the common overrepresented terms of GO biological process of *A. thaliana* and *P. cheesemanii* in responding to cold, salt, and UV-B radiation stress. (a) 84 common overrepresented GO terms in responding to cold stress were clustered with 14 representatives of GO biological processes. (b) 26 common overrepresented GO terms in responding to salt stress were clustered with 4 representatives of GO biological processes. (c) 65 common overrepresented GO terms in responding to UV-B radiation were clustered with 14 representatives of GO biological processes. Semantic space X and Y: no intrinsic meaning; uniqueness: measure whether the term is an outlier compared to the list. Namely, the negative of average similarity of a term to all other terms. In REVIGO, multi-dimensional scaling was used to reduce the dimensionality of a matrix of the GO terms' pairwise semantic similarities. First, the terms were placed by using an eigenvalue decomposition of the terms' pairwise distance matrix. Then, a stress minimization step improved the agreement between the semantic similarities of the terms and their closeness in the two-dimensional space. Thus, the semantically similar GO terms should remain close together in the plot. Figure was generated from REVIGO web (http://revigo.irb.hr/) [30].

Preprints (www.preprints.org) | NOT PEER-REVIEWED | Posted: 23 May 2023 doi:10.20944/preprints202305.1588.v1

2.6. Identification of unique biological processes in A. thaliana and P. cheesemanii responses to three stresses

To achieve an overall picture of specific responses of each species, unique overrepresented terms for *A. thaliana* and *P. cheesemanii* biological processes in each stress response were selected for REVIGO analysis as described in Materials and methods. **Figure 8** shows the resulting six scatter plots, representing the unique cold, salt and UV-B radiation response set for *A. thaliana* and *P. cheesemanii*. The *A. thaliana* cold-response set is largely encompassed by that of *P. cheesemanii* (**Figure 6**) and in **Figure 8a** this is reflected by few unique representative terms for *A. thaliana*: notably, 'Jasmonic acid metabolic process', 'Negative regulation of ethylene-activated signalling pathway' and 'Hyperosmotic salinity response'. The unique *P. cheesemanii* response set is much larger and includes 'Cell wall organisation or biogenesis', 'Positive regulation of cell communication' and 'L-phenylalanine, proline, cinnamic acid, oxylipin, and glycosinolate metabolic process'. In response to salt, both species activate a similar number of unique GO terms. Major unique *A. thaliana* clusters are 'Regulation of response to biotic stimulus', 'Wax biosynthetic process' and 'Oxylipin, jasmonic acid metabolic process', while those of *P. cheesemanii* include 'Catabolic processes', 'Stomatal movement', 'Tetrapyrrole and proline catabolic process' and 'Ageing and leaf senescence' (**Figure 8b**). Upon exposure to UV-B radiation, *A. thaliana* responds with 'Photosynthesis', 'Response to red light', 'Indole glucosinolate metabolic process', 'Defence response by callose deposition in cell wall', 'Embryo development' and several stress-related hormone metabolic processes, while unique *P. cheesemanii* responses are "Wound healing', 'Regeneration', 'Positive regulation of flavonoid biosynthetic process', 'Maltose metabolic process' and 'Anthocyanin-containing compound cinnamic acid, galactose, chlorophyll, and L-phenylalanine biosynthetic process' (**Figure 8c**).

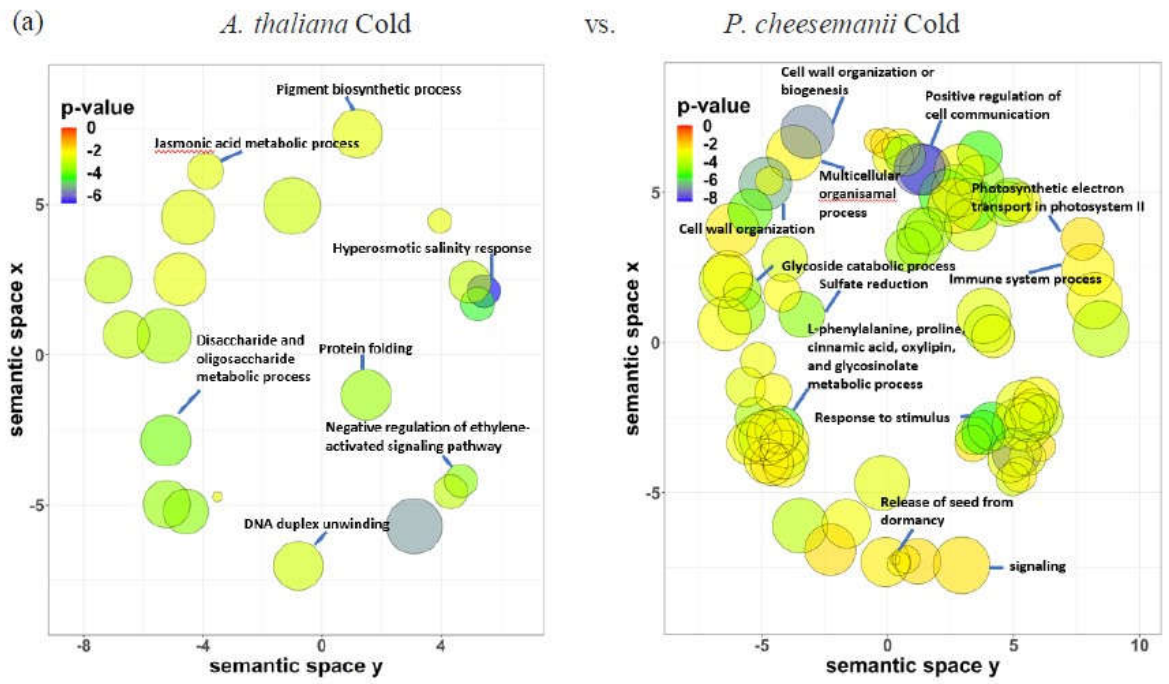

Preprints (www.preprints.org) | NOT PEER-REVIEWED | Posted: 23 May 2023 doi:10.20944/preprints202305.1588.v1

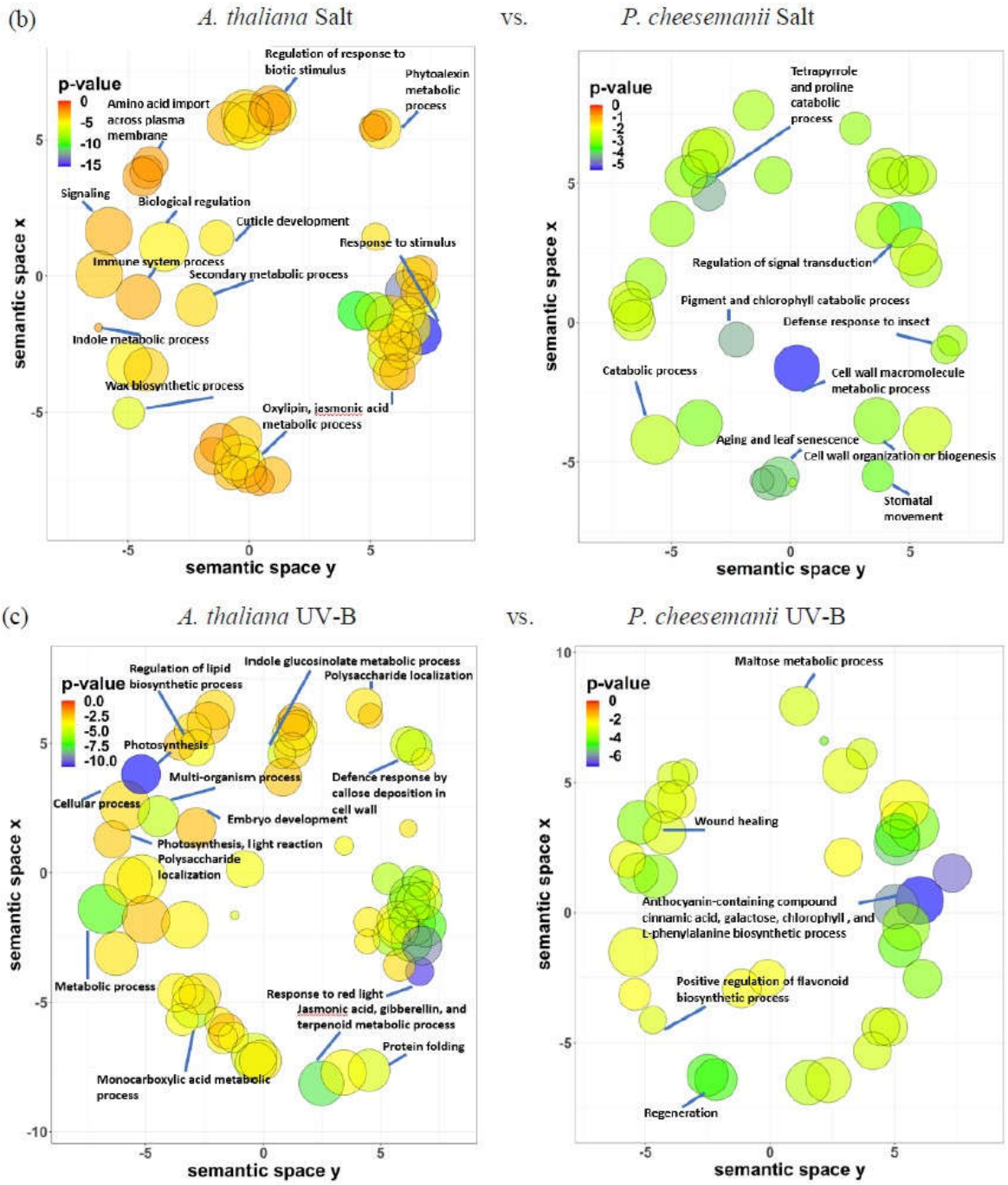

Figure 8. Unique overrepresented terms of GO biological process of *A. thaliana* and *P. cheesemanii* in response to cold, salt and UV-B radiation stress. Clustering of the unique overrepresented terms of GO biological process of *A. thaliana* and *P. cheesemanii* in responding to cold, salt, and UV-B radiation stress. (a) *A. thaliana* Cold vs *P. cheesemanii* Cold: 32 and 150 unique overrepresented GO terms of *A. thaliana* and *P. cheesemanii* in responding to cold stress were clustered with 7 and 12 representatives of GO biological processes. (b) *A. thaliana* Salt vs *P. cheesemanii* Salt: 90 and 52 unique overrepresented GO terms of *A. thaliana* and *P. cheesemanii* in responding to salt stress were clustered with 11 and 9 representatives of GO biological processes. (c) *A. thaliana* UV-B vs *P. cheesemanii* UV-B: 114 and 57 unique overrepresented GO terms of *A. thaliana* and *P. cheesemanii* in responding to UV-B radiation were clustered with 13 and 5 representatives of GO biological processes. Semantic space X and Y: no intrinsic meaning; uniqueness: measure whether the term is an outlier compared to the list. Namely, the negative of average similarity of a term to all other terms. In REVIGO, multi-dimensional scaling was used to reduce the dimensionality of a matrix of the GO terms' pairwise semantic similarities. First, the terms were placed by using an eigenvalue decomposition of the terms' pairwise

 doi:10.20944/preprints202305.1588.v1

distance matrix. Then, a stress minimization step improved the agreement between the semantic similarities of the terms and their closeness in the two-dimensional space. Thus, the semantically similar GO terms should remain close together in the plot. Figure was generated from REVIGO web (http://revigo.irb.hr/) [30].

3. Discussion

Plants must respond to a wide range of abiotic and biotic environmental stresses and different plant species have developed unique strategies for dealing with these challenges [31–34]. *P. cheesemanii* is a close relative of *A. thaliana*, and its tetraploid genome may have contributed to its ability to survive in a wide range of habitats. The work presented here aimed to detect unique stress response pathways in *P. cheesemanii*. Both species showed similarity in the number of responsive genes upregulated and downregulated under different stresses, with the exception that UV-B radiation downregulated much fewer genes in *P. cheesemanii* (**Table 1** and **Figure 1**), and in terms of overrepresented GO terms, *A. thaliana* induced more responses to this stress. In addition, *P. cheesemanii* displayed a broader response to cold stress, as compared to the other two stresses (**Figure 3**). These findings suggest that *A. thaliana* and *P. cheesemanii* induce some similar responses to each stress, but that there should also be unique stress-responsive processes in each species.

3.1. Classical stress responsive processes are conserved in both A. thaliana and P. cheesemanii

General plant stress-responses have been identified through analyses of plant stress transcriptomes and include the response to stimulus, regulation of response to stimulus, multi-organism process, biological regulation and signalling [10,35–37]. Unsurprisingly, these processes were found in both *A. thaliana* and *P. cheesemanii* responding to multiple stresses (**Figure 7**). For instance, three out of four overrepresented biological processes (multi-organism process, response to stimulus, and response to endogenous stimulus) induced by salt stress in both *A. thaliana* and *P. cheesemanii*, were induced by cold and UV-B stress as well. Only the regulation of the abscisic acid-activated signalling pathway was specific to salt stress in both plant species (**Figure 7b**).

Cold stress induced 13 common biological processes in both *A. thaliana* and *P. cheesemanii*. These included metabolic processes of trehalose, phenylpropanoid and oxylipin and rhythmic process, with the latter being highly specific for cold stress (**Figures 4** and **7a**). The circadian rhythm is coordinated with environmental signals to maintain plant fitness and survival via various hormone pathways and contribute to regulation of seed germination, leaf growth, photosynthesis and flowering [38–40]. The circadian rhythm regulates abiotic stress responses in a wide range of plant, including Arabidopsis, soybean, barley and rice [41–45]. Key circadian clock regulators, CCA1, LHY, CHE, TIC and TOC1, regulate stress responses via crosstalk with salicylic acid, jasmonic acid and ethylene signalling pathways [46,47]. *TIMING OF CAB EXPRESSION 1* (*TOC1*) can be induced by ABA treatment, and then contribute to ABA signalling induction [48]. Overexpressed *TOC1* resulted in drought hypersensitivity due to reduced stomatal closure [48]. The circadian clock furthermore regulates the extent of induction of *C-repeat Binding Factor 1/Dehydration Responsive Element Binding 1* (*CBF1/DREB1*) family of transcription factors, which contribute to cold tolerance [49]. The putative MYB transcription factor, *Cold induced MYB* (*CMYB1*) was found to respond to circadian rhythm in rice leaves at different developmental stages [50]. Induction of secondary metabolism is another common cold response in plants, and genes involved in trehalose, oxylipin and phenylpropanoid biosynthesis were upregulated in *P. cheesemanii* and *A. thaliana* in this study. Notably, these metabolites interact with circadian rhythm and hormone pathways [51–53]. Moreover, flavonoids influence the expression of circadian clock genes as found by RNA-seq analysis of an Arabidopsis flavonoid biosynthesis mutant [54]. Elevated trehalose biosynthesis increased drought, salt, cold, and heat tolerance in tobacco, potato, Arabidopsis and rice [55–57]. In *A. thaliana*, trehalose also interacts with JA and SA signalling after heat stress via multiprotein bridging factor 1c (MBF1c), a protein involved in controlling thermotolerance [58]. In maize, JA-deficient mutants revealed that wound-induced oxylipin responses are positively regulated by JA signalling [52]. In addition, other secondary metabolites, phenylpropanoids, were induced by salinity, drought, temperature and UV

 doi:10.20944/preprints202305.1588.v1

radiation stress. The downstream phenolic compounds of phenylpropanoid metabolism in turn scavenge stress-causing free radicals like $^1O_2$, O_2^{2-}, OH^-, thereby protecting plant membranes from stress-induced peroxidation damage [59,60].

Both in *A. thaliana* and *P. cheesemanii*, UV-B radiation impacted pathways involved in metabolism of L-ascorbic acid, L-phenylalanine, and chorismate from aromatic amino acid metabolic process (**Figure 7c**). Besides their structural role in proteins, phenylalanine, tyrosine and tryptophan are precursors of a number of phytohormones such as auxin and SA as well as aromatic secondary metabolites in plants and micro-organisms [61]. Phenylalanine can be deaminated by phenylalanine ammonia-lyase to produce phenylpropanoid compounds like flavonoids, anthocyanins, flavonols, and flavones [62]. Flavonoids are important pigments that protect against UV-B-induced damage because of their antioxidant capacity and absorbing UV radiation capacity [63]. In addition, genes involved in L-ascorbic acid (vitamin C) biosynthesis were impacted by UV-B radiation in both *A. thaliana* and *P. cheesemanii* (**Figure 7c**), and also in other plant species [64,65]. In cucumber seedlings, low-fluence UV-B radiation (20 μW cm^{-2}) elevated L-ascorbic acid abundance and its biosynthesis genes (*CsGLDH*, *CsMIOX1*, *CsAO2*, *CsAO4*, *CsAPX5*, CsGR1, and *CsDHAR1*) and, light-responsive elements were identified in their promoter regions [64]. Thus, biosynthesis of secondary metabolites appears a conserved strategy to cope with UV-B radiation.

In conclusion, a number of widely studied plant stress processes are highly conserved in *A. thaliana* and *P. cheesemanii* as well. This suggests that these responses likely function in adapting generic processes such as growth and development in many plant species, in order to minimise the impact of the stresses and provide time for plants to adapt to the stress and finish their lifecycle.

3.2. Unique cold, salt, and UV-B-radiation responses in A. thaliana and P. cheesemanii

Plants cope with challenging temperatures by adopting different strategies, one of which is the accumulation of low molecular weight carbohydrates (LMWC) [66]. We found that cold stress induces genes involved in biosynthesis of LMWC metabolites (oligosaccharides) in *A. thaliana* uniquely (**Figure 8a**). Galactinol synthase (GolS) catalyses the first step of the biosynthesis of the raffinose family of oligosaccharides (RFO) and overexpression of *GolS*, increases endogenous galactinol and raffinose, and improves drought tolerance in rice [67]. Its overexpression also increases the tolerance of transgenic plants to osmotic and salinity stresses, and increased levels of galactose and raffinose were found in a chilling-tolerant genotype of *Oryza sativa* after cold stress [68,69]. RFOs likely play a role in reactive oxygen species (ROS) scavenging under stress [70]. Oligosaccharides themselves can also trigger various stress-related signalling pathways [71–73]. Treatment with chitosan oligosaccharides elevates JA content in multiple plant species and the expression of JA-related genes in *Brassica napus* [74–77]. A study of *jar1* (JA-deficient), *NahG*, and *sid2* (SA-deficient) mutants in Arabidopsis suggested the involvement of both SA and JA signalling in chitosan oligosaccharide-induced resistance to *Pseudomonas syringae* pv. *tomato* DC3000 [78]. It could be the reason for 'Jasmonic acid metabolic process' and 'Negative regulation of ethylene activated signalling pathway' in *A. thaliana* unique responses to cold stress in this study (**Figure 8a**). In contrast, the responses of *P. cheesemanii* to cold stress included many more overrepresented terms for GO biological processes relative to those in responses to salt and UV-B radiation (**Figure 3**), implying the complexity of *P. cheesemanii* cold responses. Under cold stress, the responses to multiple plant hormones, including salicylic acid, ethylene and gibberellin, as well as a couple of stress-related metabolites indeed have been found in *P. cheesemanii* cold response (**Figures 5** and **8a**). Another noticeable process was glucosinolate metabolism and relevant processes (glycoside catabolic process and sulfate reduction). Glucosinolates are a class of glycosinolates whose sugar component is glucose and which are primarily found in Brassicaceae [79]. The accumulation of glucosinolates is induced by a variety of abiotic stresses such as salinity, drought, temperature and nutritional deficiencies [80–83]. Arabidopsis TU8 mutants exhibit a deficiency in glucosinolate metabolism and display less tolerance to high temperatures, while exogenous application of glucosinolate derivatives strengthens the heat tolerance of *A. thaliana* plants [84,85]. However, there was little evidence so far to support a role for glycosinolate metabolism under low temperatures. In contrast, here we identified

 doi:10.20944/preprints202305.1588.v1

glycosinolate metabolism as a unique cold response in *P. cheesemanii* (**Figure 8a**). It might be a stress-acclimating strategy similar to that of glucosinolate-induced heat tolerance, and this hypothesis would be interesting to follow up in further studies.

It has been reported that wax biosynthesis responds to salinity in a variety of plant species, which also has been found in this study [86–88]. Stress-induced wax biosynthesis has been linked to enhanced plant tolerance to abiotic stresses like low temperature and drought [89,90]. In this study, it could be associated with cuticle development in *A. thaliana*'s unique salt response as waxes are main components of the plant cuticle [91]. The cuticle plays a role in protection against water loss and its biosynthesis is responsive to environmental stress [92]. Salt stress causes accumulation of alcohols, which are wax components, and this may stimulate sugar beet growth [93]. The *A. thaliana shine* gain-of-function mutant displays increased and altered wax composition accompanied by increased cuticle permeability, reduced stomatal density and drought tolerance [94]. Similarly, the AP2 domain-containing putative transcription factor gene *WXP1* of *Medicago truncatula* can increase wax production and confer drought tolerance in *Medicago sativa* [95]. Alteration of the cuticle is widely reported in response to salt and drought stress, but, interestingly, GO terms related to this process were not overrepresented in *P. cheesemanii*.

Overrepresented pigment and chlorophyll, as well as tetrapyrrole and proline catabolic processes GO terms were unique in the *P. cheesemanii* salt response (**Figure 8b**). It was reported that foliar application of the tetrapyrrole precursor 5-aminolevulinic acid (ALA) onto salt-stressed *Brassica napus* seedlings increases chlorophyll and proline abundance and improves tolerance to salt [96]. The concentration of the tetrapyrrole chlorophyll was reduced under salt stress, resulting from a declined leaf water potential that limited photosynthetic rate and disrupted the biosynthesis of chlorophyll [96]. Elevated proline abundance is a salt-induced phenomenon in many plant species, including pepper, maize, melon, and sorghum, and it alleviates the effect of salinity stress in a number of ways, including an inhibition of stomatal opening [97–101]. Of note, the GO term 'Stomatal movement' was overrepresented in *P. cheesemanii* in response to salt stress (**Figure 8b**). Two major responses to salt and the related drought stress are alteration of the cuticle and biosynthesis of proline. Curiously, the former appears to be working only in *A. thaliana* and the latter only in *P. cheesemanii*. This suggest an important evolutionary deviation between these related species and it will be interesting to discover the functional and evolutionary basis of this difference.

A unique UV-B radiation response in *A. thaliana* was the enrichment of GO terms related to protecting actions like callose-related cell wall defence (′Polysaccharide localization′) (**Figure 8c**). This may also contribute to plants' acquired resistance to biotic stresses following UV-B radiation [102]. In *A. thaliana*, exposure to sub-lethal UV-C radiation increased the production of callose [103], and UV-B radiation induced callose ring formation and cell wall thickening of the upper part of the trichome [104]. Interestingly, GO terms related to glucosinolate metabolism were also impacted by UV-B radiation in *A. thaliana*, uniquely (**Figure 8c**). Glucosinolate-dependent callose deposition is part of the Arabidopsis innate immune response against microbial pathogens [105]. Derivates derived from glucosinolate hydrolysis were suggested to function as insect feeding and oviposition deterrents in insect resistance; they also contribute to microbe-associated molecular pattern-mediated defence as signalling molecules [106,107]. While callose-related cell wall defence is correlated with pathogen tolerance, callose deposition was also observed in response to abiotic stress, with unknown physiological and molecular mechanisms [108]. Therefore, our observations support the existence of cross-tolerance to biotic and abiotic stresses in plants [109]. After UV-B radiation treatment of *P. cheesemanii*, the enrichment network analysis identified a unique cluster related to anthocyanin biosynthesis and included the regulation of L-phenylalanine (biosynthetic precursor of anthocyanin) and anthocyanin metabolism (**Figure 8c**). This observation further implied an important role for anthocyanins in *P. cheesemanii* stress responses (**Figure 5**). Anthocyanins are a widely distributed group of water-soluble flavonoid pigments, and their biosynthesis involves more steps than those of flavone and flavonol biosynthesis [110]. Coupled with steroid metabolism, anthocyanin accumulation was associated with reduced membrane damage in other plant species and this could help stabilise membrane systems and minimise the ROS damage caused by UV-B radiation [111] in

 doi:10.20944/preprints202305.1588.v1

P. cheesemanii (**Figures 7c** and **8c**). In conclusion, the unique UV-B radiation response in *A. thaliana* suggests that changes at the cell, organ and whole plant level help adapt the plant to UV-B radiation, while in *P. cheesemanii* anthocyanin production may be a main strategy to cope with this stress.

While *A. thaliana* and *P. cheesemanii* share common stress responses, they also display considerable differences, even though they are evolutionary relatively closely related. The natural habitat of the two species is quite different [7] and our results suggest that plants evolve unique stress response pathways quickly. A better understanding of the shared and unique stress-responsive pathways of *A. thaliana* and *P. cheesemanii* could help to model common stress responses in all plant species but also provides insight into the range of potential responses that help mitigate environmental stress.

4. Materials and methods

4.1. Plant growth and stress treatments

Seeds of *P. cheesemanii* Kingston (geographical coordinates in decimal degrees −45.3273, 168.7078) was provided by Dr. Claudia Voelckel (Max Planck Institute for Chemical Ecology, Jena, Germany) and Dr. Peter Heenan (Wildland Consultants Ltd., Rotorua, New Zealand). Seeds of *Arabidopsis thaliana* Heynh. accession Col-0 was obtained from the Arabidopsis Biological Resource Center (ABRC; https://abrc.osu.edu). Seeds of both species were sown and germinated in wet Seed Raising Mix® soil from Daltons (Matamata, New Zealand) and seedlings were grown under a 16-h light (200 µmol $m^{-2}s^{-1}$ cool-white fluorescent tube)/8-h dark (long-day) regime at 22 °C. For multiple stress transcriptome profiling, seedlings were grown under a 10-h light (200 µmol $m^{-2}s^{-1}$ cool-white fluorescent lamp)/14-h dark (short-day) regime at 22 °C for six weeks (*A. thaliana*) or nine weeks (*P. cheesemanii*) **(Figure S6)**. For cold stress, plants were transferred to a 4 °C growth chamber with otherwise the same light settings. For salt stress, pots containing the plants were saturated with a 250 mM NaCl solution and excess solution was allowed to drain. The plants were transferred to the UV-B radiation chamber where they were subjected to normal white light (200 µmol $m^{-2}s^{-1}$ cool-white fluorescent tube) supplemented with 5.2 µmol $m^{-2}s^{-1}$ UV-B (290–320 nm) for UV-B treatments, while the control plants were kept under white light conditions [7]. The UV-B fluorescent tubes used in the chamber were Q-Panel 313 (Q-Lab Corp, Cleveland, OH, USA), which were wrapped in 0.13-mm-thick cellulose diacetate foil (Clarifoil; Courtaulds Ltd., Derby, UK) to remove wavelengths < 290 nm. The chamber was split into a UV-B+ zone and a UV-B− zone separated by a central curtain of UV-B opaque film (Lumivar; BPI Visqueen, Ardeer, UK). For the UV-B− zone, the UV-B tubes were wrapped in the same UV-B opaque film (Wargent et al., 2015). UV-B treatments were quantified at plant canopy height with an Optronics OL-756 UV-VIS Spectroradiometer (Optronic Laboratories, Gooch and Housego, FL, USA) equipped with integrating sphere. Spectroradiometric scans of the controlled environment chamber confirmed that the biologically effective UV dose was < 0.01 kJ $m^{-2}d^{-1}$ in the UV-B− zone **(Figure S6)**. Plants were treated one hour after the lights turned on (simulating dawn); then, five hours later (6 hours after dawn), the two largest, fully expanded mature leaves of treated and nontreated plants were collected.

4.2. Library preparation and Illumina transcriptome sequencing

Total RNA was extracted from mature leaves using a Quick-RNA MiniPrep Kit (Zymo Research, CA, USA) and treated with DNase I to remove genomic DNA contamination (**File S3**). Purified untreated and treated plant RNA was used to generate 150-bp paired-end sequencing libraries, including 12 *A. thaliana* and 12 *P. cheesemanii* samples (three biological replicates for untreated plants and each stress treatment in each plant species). Following library quality control, the libraries were sequenced on Illumina HiSeq X Ten, with 2 × 150-PE reads generating a total of ~278.2 Gb raw sequencing data. PE library construction and Illumina sequencing were performed by Novogene Limited (Beijing, China).

 doi:10.20944/preprints202305.1588.v1

4.3. Pachycladon transcriptome assembly

Sequencing adaptors were removed from sequenced reads using trim_galore v0.4.1 [112] and ribosomal RNA was filtered out by using SortMeRNA v2.1b [113]. The quality filtered reads were normalised *in silico* by using Trinity v2.5.1 [114]. Since a genome draft was assembled in our previous study, the reference genome-guided transcriptome assembly was applied [7]. However, the results from Bowtie2 and BUSCO showed that the quality of the assembled transcriptome was not optimal, as shown by a low percentage Bowtie and BUSCO alignment. Therefore, *de novo* transcriptome assembly was performed using three programs with the results compared to generate a high-quality transcriptome. Trinity, Velvet/Oases and Trans-ABySS have been suggested as providing better performance for *de novo* transcriptome assemblies [115]. The normalised read sets were then independently assembled using Trinity v2.5.1 [114], Velvet v1.1/Oases v0.2 [116,117], and Trans-ABySS v2.0.1 [118] assemblers using a range of k-mer sizes (**Table S2**). For each assembler, a popular range of k-mer sizes was selected (Trinity: 19-31-mer; Trans-ABySS: 51-63-mer; Velvet/Oases: 55-95-mer). BUSCO analyses was used to confirm whether the best assembly was achieved in the selected range. BUSCO (v3.0.2; dataset: 'embryophypta_odb9', containing 1,440 orthogroups, downloaded from http://busco.ezlab.org) [119] and the percentage of reads aligned using Bowtie2 were used as assembly quality metrics to select the Trans-ABySS assembly based on its superior completeness and accuracy. The resulting 19 assemblies were evaluated using the Bowtie alignment rate and near-universal orthologue searching (**Table S2**). Seven assemblies produced by Trans-ABySS generated higher read alignment rates (~91.08%) than those from the other two assemblers (~87.23% from Velvet/Oases and ~88.91% from Trinity). The BUSCO results generally showed high percentages of complete BUSCO across all assemblies (**Table S2**), with the exception of the 19-mer assembly from Trinity, which had higher percentages of fragmented and missing BUSCOs.

As the assemblies from the Trans-ABySS assembler outperformed those of Velvet/Oases and Trinity, based on a Bowtie evaluation, they were selected for further processing. Next, Trans-ABySS assemblies across different k-mer sizes were combined to generate the final transcript set (318,111 transcripts), which was further clustered and assembled using the CAP3 [120] assembly program. This program removed technical redundancy with 99% overlap in percentage identity and 200 bp overlap in length, resulting in 223,341 transcripts (**Table S3**). Finally, EvidentialGene: tr2aacds [121] was applied to remove redundancies and fragments, and to identify transcript splice isoforms.

4.4. Functional annotation of the Pachycladon transcriptome

Homology-based annotation was performed using BLASTP v2.6.0 [122] against the Uniprot *A. thaliana* dataset (Swissprot + TrEMBL) using the parameters best hit, E-value cut-off of 1e-20, query coverage of ≥50%, and percentage identity ≥50%. GO annotations were obtained from the Uniprot database. To annotate the final transcript set, the sequences were searched against the *A. thaliana* UniProt database using BLASTX with an E-value cut-off of 1e-5. Of the 45,911 genes, 39,949 had homologies in the UniProt database with >50% identity. These genes were mapped to 29,060 *Arabidopsis* proteins with 5,294 GO annotations. The overrepresented GO terms for biological processes were 'Carbohydrate metabolic process' (735 members), 'Cell redox homeostasis' (352 members), 'Cell wall organisation' (365 members), 'Defence response' (430 members), 'DNA integration' (493 members), 'Intracellular protein transport' (487 members), 'Protein transport' (472 members), 'Regulation of transcription, DNA-templated' (1,418 members), 'Signal transduction' (415 members) and 'Translation" (960 members) (**File S2**). There were 78% transcripts which could be annotated against the *A. thaliana* protein database, as expected, suggesting that the assembled transcriptome was suitable for downstream analysis.

4.5. Analysis of differential gene expression

To analyse differential gene expression induced by stress, the 147.1 Gb raw data with 490,400,436 raw reads from the *A. thaliana* stress response sequencing libraries was processed using trim_galore [112] to remove adaptor contamination. SortMeRNA [113] was then used to remove ribosomal RNA

 doi:10.20944/preprints202305.1588.v1

sequences from the adaptor-trimmed reads. Then, *A. thaliana* and *P. cheesemanii* reads from untreated and treated samples were mapped to the *A. thaliana* transcriptome reference (GenBank CP002684–CP002688) and the de novo assembled *P. cheesemanii* transcriptome using kallisto v0.43.1 [123], respectively. The *A. thaliana* reference used to quantify transcripts was downloaded from www.araport.org (v10). The parameters of kallisto/edgeR analysis were: counts per million (cpm) >1 (removing low count), false discovery rate (FDR) <0.05 and log of fold change (FC) ≥1. Differential gene expression was then performed using edgeR v3.26.1 [124] with default parameters.

4.6. Identification of shared and unique biological processes of species' stress responses

A number of biological processes were identified as being shared or not shared between *A. thaliana* and *P. cheesemanii* in responding to each stress. To obtain an overall structure of responses common to the species for each stress, the overrepresented terms in common between the *A. thaliana* and *P. cheesemanii* biological process in each stress response, with a 0.05 adjusted *p*-value (adjusted by Benjamini and Hochberg correction), were selected as significantly overrepresented terms. This resulted in three sets: a common cold response set; a common salt response set; and a common UV-B radiation response set. Because of the well-annotated *A. thaliana* transcriptome, *A. thaliana* genes from these three sets were used to generate three gene subsets for further GO ontology and clustering analysis. Each subset was scrutinised to identify clusters of overrepresented terms for GO biological processes and then the identified clusters were annotated functionally.

To achieve an overall picture of each species' unique response to each stress, unique overrepresented terms for *A. thaliana* and *P. cheesemanii* biological processes in each stress response (with a 0.05 adjusted *p*-value) were selected as significantly overrepresented terms. This resulted in six sets: one unique cold, salt, and UV-B radiation response set for both *A. thaliana* and *P. cheesemanii*. All genes were extracted from these six sets to generate six gene subsets. Each subset was scrutinised to identify clusters of overrepresented terms for GO biological processes and then the identified clusters were annotated functionally.

4.7. Combining weighted correlation network analysis and gene set enrichment analysis

Weighted correlation network analysis (WGCNA)-based gene modules were used as gene sets for gene set enrichment analysis (GSEA). Twelve datasets from the three stress responses (three biological replicates) in *A. thaliana* were utilised for WGCNA. The stress-responsive genes could be moulded into 11 groups; up- and downregulated genes were identified in each. GSEA v4.0.3 [125] was performed on 11 WGCNA modules in each stress and the network was then generated and visualised using EnrichmentMap and the compound spring embedder (CoSE) layout in Cytoscape v3.8.0 [126]. For the interaction network analysis of stress responses in *P. cheesemanii*, GSEA was applied to the datasets. The resulting network was also generated and visualised using EnrichmentMap and the CoSE layout in Cytoscape.

Supplementary Materials: Figure S1: Length distribution of the assembled transcripts in *P. cheesemanii* and BUSCOs assessment of assembled transcriptome; Figure S2: Network analysis of biological process of *A. thaliana* multiple stress-responsive transcriptomes in downregulation;Figure S3 Summary of the common overrepresented terms of GO biological process of *A. thaliana* and *P. cheesemanii* in responding to cold stress; Figure S4 Summary of the common overrepresented terms of GO biological process of *A. thaliana* and *P. cheesemanii* in responding to salt stress; Figure S5 Summary of the common overrepresented terms of GO biological process of *A. thaliana* and *P. cheesemanii* in responding to UV-B radiation stress; Figure S6 Five-hour stress treatment of six-week-old *A. thaliana* and nine-week-old *P. cheesemanii* plants for quantification of transcript abundance and multiple stress transcriptome profiling; **Table S1. Summary of read data for *P. cheesemanii* stress transcriptome**; **Table S2. Assessment of transcriptome assemblies generated by multiple assemblers; Table S3. Summary statistics for transcriptome assembly**, and Dr. Peter Heenan (Wildland Consultants Ltd, Rotorua, New Zealand) for providing *P. cheesemanii* seeds. The authors would also like to acknowledge the help from Massey Genome Service.

Author Contributions: P.D., J.P. and R.M. conceived the idea. P.D., J.P., R.M., T.G., Y.D, and B.M.-R. designed the study. Y.D. performed the experiments with Pachycladon and *A. thaliana* accessions. Y.D. and S.G. performed

the computational analysis of the RNA-seq data. J.J.W. designed the UV-B radiation experiments. P.D., R.M., B.M.-R. and T.G. supervised the research. Y.D., S.G., B.M.-R., and P.D. wrote the manuscript, which was corrected and approved by all authors.

Funding: This project has received funding from the European Union's Horizon 2020 research and innovation programme under grant agreement no. 642901 (CropStrengthen), project PlantaSYST (SGA-CSA No. 739582 under FPA No. 664620), and the European Regional Development Fund through the Bulgarian "Science and Education for Smart Growth" Operational Programme (project BG05M2OP001-1.003-001-C01).

Institutional Review Board Statement: Not applicable.

Informed Consent Statement: Not applicable.

Data availability Statement: Publicly available datasets were analyzed in this study. This data can be found here: the NCBI Sequencing Read Archive (SRA), BioProject ID PRJNA956584.

Acknowledgments: Authors thank Claudia Voelckel (MPI for Chemical Eology, Jena, Germa.

Conflicts of Interest: The authors declare that they have no competing interests.

References

1. Hasanuzzaman, M.; Nahar, K.; Alam, Md.; Roychowdhury, R.; Fujita, M. Physiological, Biochemical, and Molecular Mechanisms of Heat Stress Tolerance in Plants. *Int. J. Mol. Sci.* **2013**, *14*(5), 9643–9684. https://doi.org/10.3390/ijms14059643
2. Hasegawa, P. M.; Bressan, R. A.; Zhu, J.-K.; Bohnert, H. J. Plant cellular and molecular responses to high salinity. *Annu. rev. plant physiol. plant mol. biol.* **2000**, *51*(1), 463–499. https://doi.org/10.1146/annurev.arplant.51.1.463
3. Misra, A. N.; Biswal, A. K.; Misra, M. Physiological, biochemical and molecular aspects of water stress responses in plants, and the bio-technological applications. *Proc. Natl. Acad. Sci. India. Sect. B* **2002**, *72*(2), 115-134.
4. Shanker, A.; Venkateswarlu, B. Abiotic Stress in Plants: Mechanisms and Adaptations. BoD–Books on Demand; IntechOpen: Norderstedt, Germany, **2011**; p. 22.
5. Hasanuzzaman, M.; Nahar, K.; Fujit, M. Extreme Temperature Responses, Oxidative Stress and Antioxidant Defense in Plants. In *Abiotic Stress—Plant Responses and Applications in Agriculture*; InTechOpen: London, UK, **2013**; pp. 169–205. https://doi.org/10.5772/54833
6. Wang, X.; Li, W.; Li, M.; Welti, R. Profiling lipid changes in plant response to low temperatures. *Physiol. Plant.* **2006**, *126*(1), 90-96.
7. Dong, Y.; Gupta, S.; Sievers, R.; Wargent, J. J.; Wheeler, D.; Putterill, J.; Macknight, R.; Gechev, T.; Mueller-Roeber, B.; Dijkwel, P. P. Genome draft of the Arabidopsis relative *Pachycladon cheesemanii* reveals novel strategies to tolerate New Zealand's high ultraviolet B radiation environment. *BMC Genom.* **2019**, *20*(1), 838. https://doi.org/10.1186/s12864-019-6084-4
8. Rabbani, M. A.; Maruyama, K.; Abe, H.; Khan, M. A.; Katsura, K.; Ito, Y.; Yoshiwara, K.; Seki, M.; Shinozaki, K.; Yamaguchi-Shinozaki, K. Monitoring Expression Profiles of Rice Genes under Cold, Drought, and High-Salinity Stresses and Abscisic Acid Application Using cDNA Microarray and RNA Gel-Blot Analyses. *Plant Physiol.* **2003**, *133*(4), 1755–1767. https://doi.org/10.1104/pp.103.025742
9. Rensink, W. A.; Iobst, S.; Hart, A.; Stegalkina, S.; Liu, J.; Buell, C. R. Gene expression profiling of potato responses to cold, heat, and salt stress. *Funct. Integr. Genom.* **2005**, 5(4), 201–207. https://doi.org/10.1007/s10142-005-0141-6
10. Cohen, S. P.; Leach, J. E. Abiotic and biotic stresses induce a core transcriptome response in rice. *Sci. Rep.* **2019**, 9(1), 6273. https://doi.org/10.1038/s41598-019-42731-8
11. Sharma, R.; Singh, G.; Bhattacharya, S.; Singh, A. Comparative transcriptome meta-analysis of *Arabidopsis thaliana* under drought and cold stress. *PLoS One* **2018**, *13(9), e0203266*. https://doi:10.1371/journal.pone.0203266
12. Zhu, J.K. Salt and drought stress signal transduction in plants. *Annu. Rev. Plant Biol.* **2002**, *53*(1), 247–273. https://doi.org/10.1146/annurev.arplant.53.091401.143329
13. Pan, Y.; Wu, L. J.; & Yu, Z. L. Effect of salt and drought stress on antioxidant enzymes activities and SOD isoenzymes of liquorice (*Glycyrrhiza uralensis Fisch*). *Plant Growth Regul.* **2006**, *49*(2), 157-165. https://link.springer.com/article/10.1007/s10725-006-9101-y
14. Sun, C. X.; Li, M. Q.; Gao, X. X.; Liu, L. N.; Wu, X. F.; Zhou, J. H. Metabolic response of maize plants to multi-factorial abiotic stresses. *Plant Biol. (Stuttg.)* **2016**, *18 Suppl 1, 120-129*. https://doi:10.1111/plb.12305
15. Ni, L.; Wang, Z.; Guo, J.; Pei, X.; Liu, L.; Li, H.; ... Gu, C. Full-Length Transcriptome Sequencing and Comparative Transcriptome Analysis to Evaluate Drought and Salt Stress in Iris lactea var. chinensis. *Genes (Basel)* **2021**, *12(3)*. https://doi:10.3390/genes12030434

16. Xu, Y.; Magwanga, R. O.; Jin, D.; Cai, X.; Hou, Y.; Juyun, Z.; ... Zhou, Z. Comparative transcriptome analysis reveals evolutionary divergence and shared network of cold and salt stress response in diploid D-genome cotton. *BMC Plant Biol.* **2020**, *20(1), 518*. https://doi:10.1186/s12870-020-02726-4
17. Dai, Q.; Yan, B.; Huang, S.; Liu, X.; Peng, S.; Miranda, M. L. L.; Chavez, A. Q.; Vergara, B. S.; Olszyk, D. M. Response of oxidative stress defense systems in rice (Oryza sativa) leaves with supplemental UV-B radiation. *Physiol. Plant.* **1997**, 101(2), 301–308. https://doi.org/10.1111/j.1399-3054.1997.tb01000.x
18. Kim, B. C.; Tennessen, D. J.; Last, R. L. UV-B-induced photomorphogenesis in *Arabidopsis thaliana*. *Plant J.* **1998**, 15(5), 667–674. https://doi.org/10.1046/j.1365-313x.1998.00246.x
19. Raghuvanshi, R.; Sharma, R. K. Response of two cultivars of *Phaseolus vulgaris* L. (French beans) plants exposed to enhanced UV-B radiation under mountain ecosystem. *Environ. Sci. Pollut. Res.* **2016**, *23*(1),831–842. https://doi.org/10.1007/s11356-015-5332-7
20. Vyšniauskienė, R.; Rančelienė, V. Effect of UV-B radiation on growth and antioxidative enzymes activity in Lithuanian potato (*Solanum tuberosum L.*) cultivars. *Zemdirbyste-Agriculture* **2014**, 101(1), 51–56. https://doi.org/10.13080/z-a.2014.101.007
21. Casati, P.; Walbot, V. Rapid transcriptome responses of maize (Zea mays) to UV-B in irradiated and shielded tissues. *Genome Biol.* **2004**, *5*(3), R16. https://doi.org/10.1186/gb-2004-5-3-r16
22. Gil, M.; Pontin, M.; Berli, F.; Bottini, R.; Piccoli, P. Metabolism of terpenes in the response of grape (*Vitis vinifera L.*) leaf tissues to UV-B radiation. *Phytochem.* **2012**, *77*, 89–98. https://doi.org/10.1016/j.phytochem.2011.12.011
23. Wang, H.; Li, J.; Tao, W.; Zhang, X.; Gao, X.; Yong, J.; Zhao, J.; Zhang, L.; Li, Y.; Duan, J. *Lycium ruthenicum* studies: Molecular biology, Phytochemistry and pharmacology. *Food Chem.* **2018**, *240*, 759–766. https://doi.org/10.1016/j.foodchem.2017.08.026
24. Kilian, J.; Whitehead, D.; Horak, J.; Wanke, D.; Weinl, S.; Batistic, O.; D'Angelo, C.; Bornberg-Bauer, E.; Kudla, J.; Harter, K. The AtGenExpress global stress expression data set: Protocols, evaluation and model data analysis of UV-B light, drought and cold stress responses. *Plant J.* **2007**, *50*(2), 347–363. https://doi.org/10.1111/j.1365-313X.2007.03052.x
25. Heenan, P.; Mitchell, A. Phylogeny, biogeography and adaptive radiation of Pachycladon (Brassicaceae) in the mountains of South Island, New Zealand. *J. Biogeogr.* **2003**, 30(11), 1737-1749. https://onlinelibrary.wiley.com/doi/abs/10.1046/j.1365-2699.2003.00941.x
26. Burghelea, C.; Zaharescu, D.; Dontsova, K.; Maier, R.; Huxman, T.; Chorover, J. Mineral nutrient mobilization by plants from rock: influence of rock type and arbuscular mycorrhiza. *Biogeochemistry* **2015**, 124, 187-203. https://link.springer.com/article/10.1007/s10533-015-0092-5
27. Hoffmann, M. H. Biogeography of *Arabidopsis thaliana* (L.) heynh. (Brassicaceae). *J. Biogeogr.* **2002**, 29(1), 125-134. https://onlinelibrary.wiley.com/doi/abs/10.1046/j.1365-2699.2002.00647.x
28. Joly, S.; Heenan, P. B.; Lockhart, P. J. A Pleistocene inter-tribal allopolyploidization event precedes the species radiation of Pachycladon (Brassicaceae) in New Zealand. *Mol. Phylogenet. Evol.* **2009**, 51(2), 365-372. doi:10.1016/j.ympev.2009.02.015
29. Li, J.; Witten, D. M.; Johnstone, I. M.; Tibshirani, R. Normalization, testing, and false discovery rate estimation for RNA-sequencing data. *Biostatistics* **2012**, *13*(3), 523–538. https://doi.org/10.1093/biostatistics/kxr031
30. Supek, F.; Bošnjak, M.; Škunca, N.; Šmuc, T. REVIGO Summarizes and Visualizes Long Lists of Gene Ontology Terms. *PLoS ONE* **2011**, *6*(7), e21800. https://doi.org/10.1371/journal.pone.0021800
31. Abla, M.; Sun, H.; Li, Z.; Wei, C.; Gao, F.; Zhou, Y.; Feng, J. Identification of miRNAs and Their Response to Cold Stress in Astragalus Membranaceus. *Biomolecules* **2019**, *9*(5), 182. https://doi.org/10.3390/biom9050182
32. Agurla, S.; Gahir, S.; Munemasa, S.; Murata, Y.; and Raghavendra, A. S. Mechanism of stomatal closure in plants exposed to drought and cold stress. *Adv. Exp. Med. Biol.* **2018**, *1081*, 215–232. https://doi.org/10.1007/978-981-13-1244-1_12
33. Fei, J.; Wang, Y.; Cheng, H.; Su, Y.; Zhong, Y.; Zheng, L. Cloning and characterization of KoOsmotin from mangrove plant Kandelia obovata under cold stress. *BMC Plant Biol.* **2021**, 21(1), 10. https://doi.org/10.1186/s12870-020-02746-0
34. Zeng, Z.; Zhang, W.; Marand, A. P.; Zhu, B.; Buell, C. R.; Jiang, J. Cold stress induces enhanced chromatin accessibility and bivalent histone modifications H3K4me3 and H3K27me3 of active genes in potato. *Genome Biol.* **2019**, *20*(1), 123. https://doi.org/10.1186/s13059-019-1731-2
35. Jiang, C.; Li, X.; Zou, J.; Ren, J.; Jin, C.; Zhang, H.; Yu, H.; Jin, H. Comparative transcriptome analysis of genes involved in the drought stress response of two peanut (*Arachis hypogaea* L.) varieties. *BMC Plant Biol.* **2021**, *21*(1), 64. https://doi.org/10.1186/s12870-020-02761-1
36. Kashyap, S. P.; Prasanna, H. C.; Kumari, N.; Mishra, P.; Singh, B. Understanding salt tolerance mechanism using transcriptome profiling and de novo assembly of wild tomato Solanum chilense. *Sci. Rep.* **2020**, *10*(1), 15835. https://doi.org/10.1038/s41598-020-72474-w

37. Li, X.; Li, M.; Zhou, B.; Yang, Y.; Wei, Q.; Zhang, J. Transcriptome analysis provides insights into the stress response crosstalk in apple (Malus × domestica) subjected to drought, cold and high salinity. *Sci. Rep.* **2019**, *9*(1), 9071. https://doi.org/10.1038/s41598-019-45266-0
38. Inoue, K.; Araki, T.; Endo, M. Circadian clock during plant development. *J. Plant Res.* **2018**, *131*(1), 59–66. https://doi.org/10.1007/s10265-017-0991-8
39. Singh, M.; Mas, P. A Functional Connection between the Circadian Clock and Hormonal Timing in Arabidopsis. *Genes* 2018, 9(12), 567. https://doi.org/10.3390/genes9120567
40. Xu, X.; Yuan, L.; Yang, X.; Zhang, X.; Wang, L.; Xie, Q. Circadian clock in plants: Linking timing to fitness. *J. Integr. Plant Biol.* **2022**, *64*(4), 792–811. https://doi.org/10.1111/jipb.13230
41. Andreeva, A. A.; Kudryakova, N. V.; Kuznetsov, Vl. V.; Kusnetsov, V. V. Ontogenetic, Light, and Circadian Regulation of PAP Protein Genes during Seed Germination of *Arabidopsis thaliana*. *Dokl. Biochem. Biophys.* **2021**, 500(1), 312–316. https://doi.org/10.1134/S1607672921050021
42. Blair, E. J.; Bonnot, T.; Hummel, M.; Hay, E.; Marzolino, J. M.; Quijada, I. A.; Nagel, D. H. Contribution of time of day and the circadian clock to the heat stress responsive transcriptome in Arabidopsis. *Sci. Rep.* **2019**, *9*(1), 4814. https://doi.org/10.1038/s41598-019-41234-w
43. Cao, L. The Molecular Interactions of Soybean Circadian Clock with Abiotic Stresses and Soybean Cyst Nematode (*Heterodera glycines*). Ph.D. thesis, Iowa State University, Ames, Iowa, United States, **2022**. https://www.proquest.com/docview/2309795320/abstract/1C0407289E124C0BPQ/1
44. Chang, T.; Zhao, Y.; He, H.; Xi, Q.; Fu, J.; Zhao, Y. Exogenous melatonin improves growth in hulless barley seedlings under cold stress by influencing the expression rhythms of circadian clock genes. *PeerJ* **2021**, *9*, e10740. https://doi.org/10.7717/peerj.10740
45. Lu, X.; Zhou, Y.; Fan, F.; Peng, J.; Zhang, J. Coordination of light, circadian clock with temperature: The potential mechanisms regulating chilling tolerance in rice. *J. Integr. Plant Biol.* **2020**, *62*(6), 737–760. https://doi.org/10.1111/jipb.12852
46. Cortleven, A.; Roeber, V. M.; Frank, M.; Bertels, J.; Lortzing, V.; Beemster, G. T. S.; Schmülling, T. Photoperiod Stress in *Arabidopsis thaliana* Induces a Transcriptional Response Resembling That of Pathogen Infection. *Front. Plant Sci.* **2022**, *13*, 838284. https://doi.org/10.3389/fpls.2022.838284
47. Srivastava, D.; Shamim, Md.; Kumar, M.; Mishra, A.; Maurya, R.; Sharma, D.; Pandey, P.; Singh, K. N. Role of circadian rhythm in plant system: An update from development to stress response. *Environ. Exp. Bot.* **2019**, *162*, 256–271. https://doi.org/10.1016/j.envexpbot.2019.02.025
48. Legnaioli, T.; Cuevas, J.; Mas, P. TOC1 functions as a molecular switch connecting the circadian clock with plant responses to drought. *EMBO Rep.* **2009**, *28*(23), 3745–3757. https://doi.org/10.1038/emboj.2009.297
49. Fowler, S.; Thomashow, M. F. Arabidopsis Transcriptome Profiling Indicates That Multiple Regulatory Pathways Are Activated during Cold Acclimation in Addition to the CBF Cold Response Pathway. *Plant Cell* **2002**, *14*(8), 1675–1690. https://doi.org/10.1105/tpc.003483
50. Duan, M.; Huang, P.; Yuan, X.; Chen, H.; Huang, J.; Zhang, H. *CMYB1* Encoding a MYB Transcriptional Activator Is Involved in Abiotic Stress and Circadian Rhythm in Rice. *Sci. World J.* **2014**, *2014*, 1–9. https://doi.org/10.1155/2014/178038
51. Gao, Y.; Yang, X.; Yang, X.; Zhao, T.; An, X.; Chen, Z. Characterization and expression pattern of the trehalose-6-phosphate synthase and trehalose-6-phosphate phosphatase gene families in Populus. *Int. J. Biol. Macromol.* **2021**, *187*, 9–23. https://doi.org/10.1016/j.ijbiomac.2021.07.096
52. He, Y.; Borrego, E. J.; Gorman, Z.; Huang, P.-C.; Kolomiets, M. V. Relative contribution of LOX10, green leaf volatiles and JA to wound-induced local and systemic oxylipin and hormone signature in Zea mays (maize). *Phytochem.* **2020**, 174, 112334. https://doi.org/10.1016/j.phytochem.2020.112334
53. Tyagi, K.; Maoz, I.; Kochanek, B.; Sela, N.; Lerno, L.; Ebeler, S. E.; Lichter, A. Cytokinin but not gibberellin application had major impact on the phenylpropanoid pathway in grape. *Hortic. Res.* **2021**, *8*(1), 51. https://doi.org/10.1038/s41438-021-00488-0
54. Hildreth, S. B.; Littleton, E. S.; Clark, L. C.; Puller, G. C.; Kojima, S.; Winkel, B. S. Crosstalk between flavonoids and the plant circadian clock. *BioRxiv* **2021**, 2021-07.https://doi.org/10.1101/2021.07.15.452546
55. Romero, C.; Bellés, J. M.; Vayá, J. L.; Serrano, R.; Culiáñez-Macià, F. A. Expression of the yeast trehalose-6-phosphate synthase gene in transgenic tobacco plants: Pleiotropic phenotypes include drought tolerance. *Planta* **1997**, *201*(3), 293–297. https://doi.org/10.1007/s004250050069
56. Lin, Q.; Yang, J.; Wang, Q.; Zhu, H.; Chen, Z.; Dao, Y.; Wang, K. Overexpression of the trehalose-6-phosphate phosphatase family gene AtTPPF improves the drought tolerance of *Arabidopsis thaliana*. *BMC Plant Biol.* **2019**, *19*(1), 381. https://doi.org/10.1186/s12870-019-1986-5
57. Jang, I.-C.; Oh, S.-J.; Seo, J.-S.; Choi, W.-B.; Song, S. I.; Kim, C. H.; Kim, Y. S.; Seo, H.-S.; Choi, Y. D.; Nahm, B. H.; Kim, J.-K. Expression of a Bifunctional Fusion of the *Escherichia coli* Genes for Trehalose-6-Phosphate Synthase and Trehalose-6-Phosphate Phosphatase in Transgenic Rice Plants Increases Trehalose Accumulation and Abiotic Stress Tolerance without Stunting Growth. *Plant Physiol.* **2003**, *131*(2), 516–524. https://doi.org/10.1104/pp.007237

58. Wang, X.; Du, Y.; Yu, D. Trehalose phosphate synthase 5-dependent trehalose metabolism modulates basal defense responses in *Arabidopsis thaliana*. *J. Integr. Plant Biol.* **2019**, *61*(4), 509–527. https://doi.org/10.1111/jipb.12704
59. Ahanger, M. A.; Tomar, N. S.; Tittal, M.; Argal, S.; Agarwal, R. M. Plant growth under water/salt stress: ROS production; antioxidants and significance of added potassium under such conditions. *Physiol. Mol. Biol* **2017**, *23*(4), 731–744. https://doi.org/10.1007/s12298-017-0462-7
60. Harinasut, P.; Poonsopa, D.; Roengmongkol, K.; Charoensataporn, R. Salinity effects on antioxidant enzymes in mulberry cultivar. *Sci.* **2003**, *29*(2), 109. https://doi.org/10.2306/scienceasia1513-1874.2003.29.109
61. Parthasarathy, A.; Cross, P. J.; Dobson, R. C. J.; Adams, L. E.; Savka, M. A.; Hudson, A. O. A Three-Ring Circus: Metabolism of the Three Proteogenic Aromatic Amino Acids and Their Role in the Health of Plants and Animals. *Front. Mol. Biosci.* **2018**, *5*, 29. https://doi.org/10.3389/fmolb.2018.00029
62. Kong, J.-Q. Phenylalanine ammonia-lyase, a key component used for phenylpropanoids production by metabolic engineering. *RSC Adv.* **2015**, *5*(77), 62587–62603. https://doi.org/10.1039/C5RA08196C
63. Singh, M.; Bashri, G.; Prasad, S. M.; Singh, V. P. Kinetin Alleviates UV-B-Induced Damage in Solanum lycopersicum: Implications of Phenolics and Antioxidants. *J. Plant Growth Regul.* **2019**, *38*(3), 831–841. https://doi.org/10.1007/s00344-018-9894-8
64. Liu, P.; Li, Q.; Gao, Y.; Wang, H.; Chai, L.; Yu, H.; Jiang, W. A New Perspective on the Effect of UV-B on L -Ascorbic Acid Metabolism in Cucumber Seedlings. *J. Agric. Food Chem.* **2019**, *67*(16), 4444–4452. https://doi.org/10.1021/acs.jafc.9b00327
65. Xu, Y.; Fu, X.; Lu, M.; Wei, B. A transcriptomic perspective on the effect of UV irradiation on vitamin C content in pea sprouts. *J. Food Sci. Technol.* **2022**, *42*, e09022. https://doi.org/10.1590/fst.09022
66. Megías-Pérez, R.; Hahn, C.; Ruiz-Matute, A. I.; Behrends, B.; Albach, D. C.; Kuhnert, N. Changes in low molecular weight carbohydrates in kale during development and acclimation to cold temperatures determined by chromatographic techniques coupled to mass spectrometry. *Food Res. Int.* **2020**, *127*, 108727. https://doi.org/10.1016/j.foodres.2019.108727
67. Selvaraj, M. G.; Ishizaki, T.; Valencia, M.; Ogawa, S.; Dedicova, B.; Ogata, T.; Yoshiwara, K.; Maruyama, K.; Kusano, M.; Saito, K.; Takahashi, F.; Shinozaki, K.; Nakashima, K.; Ishitani, M. Overexpression of an *Arabidopsis thaliana* galactinol synthase gene improves drought tolerance in transgenic rice and increased grain yield in the field. *Plant Biotechnol. J.* **2017**, *15*(11), 1465–1477. https://doi.org/10.1111/pbi.12731
68. Morsy, M. R.; Jouve, L.; Hausman, J.-F.; Hoffmann, L.; Stewart, J. McD. Alteration of oxidative and carbohydrate metabolism under abiotic stress in two rice (*Oryza sativa* L.) genotypes contrasting in chilling tolerance. *J. Plant Physiol.* **2007**, *164*(2), 157–167. https://doi.org/10.1016/j.jplph.2005.12.004
69. Sun, Z.; Qi, X.; Wang, Z.; Li, P.; Wu, C.; Zhang, H.; Zhao, Y. Overexpression of TsGOLS2, a galactinol synthase, in *Arabidopsis thaliana* enhances tolerance to high salinity and osmotic stresses. *Plant Physiol. Biochem.* **2013**, *69*, 82–89. https://doi.org/10.1016/j.plaphy.2013.04.009
70. Van den Ende, W.; Peshev, D. Sugars as antioxidants in plants. In *Crop Improvement under Adverse Conditions*; Springer: Dordrecht, The Netherlands, **2013**; pp. 285–307. https://doi.org/10.1007/978-1-4614-4633-0_13
71. Bolouri-Moghaddam, M. R.; Le Roy, K.; Xiang, L.; Rolland, F.; Van den Ende, W. Sugar signalling and antioxidant network connections in plant cells: Sugar signalling and antioxidant networks in plants. *FEBS J.* **2010**, *277*(9), 2022–2037. https://doi.org/10.1111/j.1742-4658.2010.07633.x
72. Shen, X.; Wang, Z.; Song, X.; Xu, J.; Jiang, C.; Zhao, Y.; Ma, C.; Zhang, H. Transcriptomic profiling revealed an important role of cell wall remodelling and ethylene signalling pathway during salt acclimation in Arabidopsis. *Plant Mol. Biol.* **2014**, *86*(3), 303–317. https://doi.org/10.1007/s11103-014-0230-9
73. Van den Ende, W.; El-Esawe, S. K. Sucrose signaling pathways leading to fructan and anthocyanin accumulation: A dual function in abiotic and biotic stress responses? *Environ. Exp. Bot.* **2014**, *108*, 4–13. https://doi.org/10.1016/j.envexpbot.2013.09.017
74. Doares, S. H.; Syrovets, T.; Weiler, E. W.; Ryan, C. A. Oligogalacturonides and chitosan activate plant defensive genes through the octadecanoid pathway. *Proc. Natl. Acad. Sci. U.S.A.* **1995**, *92*(10), 4095–4098. https://doi.org/10.1073/pnas.92.10.4095
75. Jia, X.; Zeng, H.; Bose, S. K.; Wang, W.; Yin, H. Chitosan oligosaccharide induces resistance to Pst DC3000 in Arabidopsis via a non-canonical N-glycosylation regulation pattern. *Carbohydr. Polym.* **2020**, *250*, 116939. https://doi.org/10.1016/j.carbpol.2020.116939
76. Linden, J. C.; Phisalaphong, M. Oligosaccharides potentiate methyl jasmonate-induced production of paclitaxel in Taxus canadensis. *Plant Sci.* **2000**, *158*(1–2), 41–51. https://doi.org/10.1016/S0168-9452(00)00306-X
77. Yin, H.; Li, S.; Zhao, X.; Du, Y.; Ma, X. CDNA microarray analysis of gene expression in Brassica napus treated with oligochitosan elicitor. *Plant Physiol. Biochem.* **2006**, *44*(11–12), 910–916. https://doi.org/10.1016/j.plaphy.2006.10.002
78. Jia, X.; Zeng, H.; Wang, W.; Zhang, F.; Yin, H. Chitosan Oligosaccharide Induces Resistance to *Pseudomonas syringae* pv. *Tomato* DC3000 in *Arabidopsis thaliana* by Activating Both Salicylic Acid– and Jasmonic Acid–

Mediated Pathways. *Mol. Plant Microbe Interact.* **2018**, *31*(12), 1271–1279. https://doi.org/10.1094/MPMI-03-18-0071-R

79. Wennberg, M.; Ekvall, J.; Olsson, K.; Nyman, M. Changes in carbohydrate and glucosinolate composition in white cabbage (Brassica oleracea var. Capitata) during blanching and treatment with acetic acid. *Food Chem.* **2006**, *95*(2), 226–236. https://doi.org/10.1016/j.foodchem.2004.11.057
80. Cocetta, G.; Mishra, S.; Raffaelli, A.; Ferrante, A. Effect of heat root stress and high salinity on glucosinolates metabolism in wild rocket. *J. Plant Physiol.* **2018**, *231, 261-270*. https://doi:10.1016/j.jplph.2018.10.003
81. Ljubej, V.; Radojcic Redovnikovic, I.; Salopek-Sondi, B.; Smolko, A.; Roje, S.; Samec, D. Chilling and Freezing Temperature Stress Differently Influence Glucosinolates Content in *Brassica oleracea var. acephala*. *Plants (Basel)* **2021**, *10*(7). doi:10.3390/plants10071305
82. Salehin, M.; Li, B.; Tang, M.; Katz, E.; Song, L.; Ecker, J. R.; ... Estelle, M. Auxin-sensitive Aux/IAA proteins mediate drought tolerance in Arabidopsis by regulating glucosinolate levels. *Nat. Commun.* **2019**, *10(1), 4021*. https://doi:10.1038/s41467-019-12002-1
83. Troufflard, S.; Mullen, W.; Larson, T. R.; Graham, I. A.; Crozier, A.; Amtmann, A.; Armengaud, P. Potassium deficiency induces the biosynthesis of oxylipins and glucosinolates in *Arabidopsis thaliana*. *BMC Plant Biol.* **2010**, *10,* 172. https://doi:10.1186/1471-2229-10-172
84. Hara, M.; Harazaki, A.; Tabata, K. Administration of isothiocyanates enhances heat tolerance in *Arabidopsis thaliana*. *Plant Growth Regul.* **2013**, *69*(1), 71–77. https://doi.org/10.1007/s10725-012-9748-5
85. Ludwig-Müller, J.; Krishna, P.; Forreiter, C. A Glucosinolate Mutant of Arabidopsis Is Thermosensitive and Defective in Cytosolic Hsp90 Expression after Heat Stress. *Plant Physiol.* **2000**, *123*(3), 949–958. https://doi.org/10.1104/pp.123.3.949
86. More, P.; Agarwal, P.; Joshi, P. S.; Agarwal, P. K. The JcWRKY tobacco transgenics showed improved photosynthetic efficiency and wax accumulation during salinity. *Sci. Rep.* **2019**, *9*(1), 19617. https://doi.org/10.1038/s41598-019-56087-6
87. Shepherd, T.; Wynne Griffiths, D. The effects of stress on plant cuticular waxes. *New Phytol.* **2006**, *171*(3), 469–499. https://doi.org/10.1111/j.1469-8137.2006.01826.x
88. Zhou, M.; Li, D.; Li, Z.; Hu, Q.; Yang, C.; Zhu, L.; Luo, H. Constitutive Expression of a *miR319* Gene Alters Plant Development and Enhances Salt and Drought Tolerance in Transgenic Creeping Bentgrass. *Plant Physiol.* **2013**, *161*(3), 1375–1391. https://doi.org/10.1104/pp.112.208702
89. Djemal, R.; Khoudi, H. TdSHN1, a WIN1/SHN1-type transcription factor, imparts multiple abiotic stress tolerance in transgenic tobacco. *Environ. Exp. Bot.* **2016**, *131*, 89–100. https://doi.org/10.1016/j.envexpbot.2016.07.005
90. Zhu, X.; Xiong, L. Putative megaenzyme DWA1 plays essential roles in drought resistance by regulating stress-induced wax deposition in rice. *Proc. Natl. Acad. Sci. U.S.A.* **2013**, *110*(44), 17790–17795. https://doi.org/10.1073/pnas.1316412110
91. Kunst, L.; Samuels, L. Plant cuticles shine: Advances in wax biosynthesis and export. *Curr. Opin. Plant* **2009**, *12*(6), 721–727. https://doi.org/10.1016/j.pbi.2009.09.009
92. Bi, H.; Kovalchuk, N.; Langridge, P.; Tricker, P. J.; Lopato, S.; Borisjuk, N. The impact of drought on wheat leaf cuticle properties. *BMC Plant Biol.* **2017**, *17*(1), 85. https://doi.org/10.1186/s12870-017-1033-3
93. Geng, G.; Li, R.; Stevanato, P.; Lv, C.; Lu, Z.; Yu, L.; Wang, Y. Physiological and Transcriptome Analysis of Sugar Beet Reveals Different Mechanisms of Response to Neutral Salt and Alkaline Salt Stresses. *Front. Plant Sci.* **2020**, *11*, 571864. https://doi.org/10.3389/fpls.2020.571864
94. Aharoni, A.; Dixit, S.; Jetter, R.; Thoenes, E.; van Arkel, G.; Pereira, A. The SHINE Clade of AP2 Domain Transcription Factors Activates Wax Biosynthesis, Alters Cuticle Properties, and Confers Drought Tolerance when Overexpressed in Arabidopsis. *Plant Cell* **2004**, *16*(9), 2463–2480. https://doi.org/10.1105/tpc.104.022897
95. Zhang, J.Y.; Broeckling, C. D.; Blancaflor, E. B.; Sledge, M. K.; Sumner, L. W.; Wang, Z.Y. Overexpression of WXP1, a putative Medicago truncatula AP2 domain-containing transcription factor gene, increases cuticular wax accumulation and enhances drought tolerance in transgenic alfalfa (*Medicago sativa*). *Plant J.* **2005**, *42*(5), 689–707. https://doi.org/10.1111/j.1365-313X.2005.02405.x
96. Xiong, J.L.; Wang, H.C.; Tan, X.Y.; Zhang, C.L.; Naeem, M. S. 5-aminolevulinic acid improves salt tolerance mediated by regulation of tetrapyrrole and proline metabolism in *Brassica napus* L. seedlings under NaCl stress. *Plant Physiol. Biochem.* **2018**, *124*, 88–99. https://doi.org/10.1016/j.plaphy.2018.01.001
97. Korkmaz, A.; Şirikçi, R.; Kocaçınar, F.; Değer, Ö.; Demirkırıan, A. R. Alleviation of salt-induced adverse effects in pepper seedlings by seed application of glycinebetaine. *Sci. Hortic.* **2012**, *148*, 197–205. https://doi.org/10.1016/j.scienta.2012.09.029
98. Pingle, S. N.; Suryawanshi, S. T.; Pawar, K. R.; Harke, S. N. The Effect of Salt Stress on Proline Content in Maize (Zea mays). *LAFOBA2* **2022**, 64. https://doi.org/10.3390/environsciproc2022016064
99. Sivritepe, N.; Sivritepe, H. O.; Eris, A. The effects of NaCl priming on salt tolerance in melon seedlings grown under saline conditions. *Sci. Hortic.* **2003**, *97*(3–4), 229–237. https://doi.org/10.1016/S0304-4238(02)00198-X

100. Sobahan, M. A.; Akter, N.; Ohno, M.; Okuma, E.; Hirai, Y.; Mori, I. C.; Nakamura, Y.; Murata, Y. Effects of Exogenous Proline and Glycinebetaine on the Salt Tolerance of Rice Cultivars. *Biosci. Biotechnol. Biochem.* **2012**, *76*(8), 1568–1570. https://doi.org/10.1271/bbb.120233
101. Weimberg, R.; Lerner, H. R.; Poljakoff-Mayber, A. A relationship between potassium and proline accumulation in salt-stressed Sorghum bicolor. *Physiol. Plant.* **1982**, *55*(1), 5–10. https://doi.org/10.1111/j.1399-3054.1982.tb00276.x
102. Kravets, E. A.; Zelena, L. B.; Zabara, E. P.; Blume, Ya. B. Adaptation strategy of barley plants to UV-B radiation. *Emir. J. Food Agric.* **2012**, *24*(6). https://doi.org/10.9755/ejfa.v24i6.14682
103. Mintoff, S. J. L.; Rookes, J. E.; Cahill, D. M. Sub-lethal UV-C radiation induces callose, hydrogen peroxide and defence-related gene expression in A rabidopsis thaliana. *Plant Biol* **2015**, 17(3), 703-711. https://doi.org/10.1111/plb.12286
104. Kulich, I.; Vojtíková, Z.; Glanc, M.; Ortmannová, J.; Rasmann, S.; Žárský, V. Cell wall maturation of Arabidopsis trichomes is dependent on exocyst subunit EXO70H4 and involves callose deposition. *Plant Physiol.* **2015**, 168(1), 120-131.
105. Clay, N. K.; Adio, A. M.; Denoux, C.; Jander, G.; Ausubel, F. M. Glucosinolate Metabolites Required for an *Arabidopsis* Innate Immune Response. *Science* **2009**, *323*(5910), 95–101. https://doi.org/10.1126/science.1164627
106. Ahuja, I.; Rohloff, J.; Bones, A.M. Defence mechanisms of Brassicaceae: Implications for plant-insect interactions and potential for integrated pest management. A review. *Agron. Sustain. Dev.* **2010**, 30, 311–348 https://doi.org/10.1007/978-94-007-0394-0_28
107. De Coninck, B.; Timmermans, P.; Vos, C.; Cammue, B. P. A.; Kazan, K. What lies beneath: Belowground defense strategies in plants. *Trends Plant Sci.* **2015**, *20*(2), 91–101. https://doi.org/10.1016/j.tplants.2014.09.007
108. Stass, A.; Horst, W. J. Callose in Abiotic Stress. In *Chemistry, Biochemistry, and Biology of 1-3 Beta Glucans and Related Polysaccharides*, 1st ed.; Antony Bacic, Geoffrey B. Fincher, Bruce A. Stone, Eds.; Elsevier: Oxford, UK, **2009**; pp. 499–524. https://doi.org/10.1016/B978-0-12-373971-1.00015-7
109. Foyer, C. H.; Rasool, B.; Davey, J. W.; Hancock, R. D. Cross-tolerance to biotic and abiotic stresses in plants: A focus on resistance to aphid infestation. *J. Exp. Bot.* **2016**, *67*(7), 2025–2037. https://doi.org/10.1093/jxb/erw079
110. Martin, C.; Gerats, T. Control of Pigment Biosynthesis Genes during Petal Development. *Plant Cell* **1993**, 1253–1264. https://doi.org/10.1105/tpc.5.10.1253
111. Berli, F. J.; Moreno, D.; Piccoli, P.; HESPANHOL-VIANA, L. E. A. N. D. R. O.; Silva, M. F.; BRESSAN-SMITH, R. I. C. A. R. D. O.; ... Bottini, R. Abscisic acid is involved in the response of grape (Vitis vinifera L.) cv. Malbec leaf tissues to ultraviolet-B radiation by enhancing ultraviolet-absorbing compounds, antioxidant enzymes and membrane sterols. *Plant Cell Environ.* **2010**, *33*(1): 1-10. https://doi.org/10.1111/j.1365-3040.2009.02044.x
112. Krueger F. Trim galore: a wrapper tool around Cutadapt and FastQC to consistently apply quality and adapter trimming to FastQ files. **2015**. Available from http://www.bioinformatics.babraham.ac.uk/projects/trim_galore/.
113. Kopylova, E.; Noé, L.; Touzet, H. SortMeRNA: Fast and accurate filtering of ribosomal RNAs in metatranscriptomic data. *Bioinformatics* **2012**, *28*(24), 3211–3217. https://doi.org/10.1093/bioinformatics/bts611
114. Grabherr, M. G.; Haas, B. J.; Yassour, M.; Levin, J. Z.; Thompson, D. A.; Amit, I.; Adiconis, X.; Fan, L.; Raychowdhury, R.; Zeng, Q.; Chen, Z.; Mauceli, E.; Hacohen, N.; Gnirke, A.; Rhind, N.; di Palma, F.; Birren, B. W.; Nusbaum, C.; Lindblad-Toh, K.; … Regev, A. Full-length transcriptome assembly from RNA-Seq data without a reference genome. *Nat. Biotechnol.* **2011**, *29*(7), 644–652. https://doi.org/10.1038/nbt.1883
115. Zhao, Q.Y.; Wang, Y.; Kong, Y.M.; Luo, D.; Li, X.; Hao, P. Optimizing de novo transcriptome assembly from short-read RNA-Seq data: A comparative study. *BMC Bioinform.* **2011**, *12*(S14), S2. https://doi.org/10.1186/1471-2105-12-S14-S2
116. Schulz, M. H.; Zerbino, D. R.; Vingron, M.; Birney, E. Oases: Robust de novo RNA-seq assembly across the dynamic range of expression levels. *Bioinformatics* **2012**, *28*(8), 1086–1092. https://doi.org/10.1093/bioinformatics/bts094
117. Zerbino, D. R.; Birney, E. Velvet: Algorithms for de novo short read assembly using de Bruijn graphs. *Genome Res.* **2008**, *18*(5), 821–829. https://doi.org/10.1101/gr.074492.107
118. Robertson, G.; Schein, J.; Chiu, R.; Corbett, R.; Field, M.; Jackman, S. D.; Mungall, K.; Lee, S.; Okada, H. M.; Qian, J. Q.; Griffith, M.; Raymond, A.; Thiessen, N.; Cezard, T.; Butterfield, Y. S.; Newsome, R.; Chan, S. K.; She, R.; Varhol, R.; … Birol, I. De novo assembly and analysis of RNA-seq data. *Nat. Methods* **2010**, *7*(11), 909–912. https://doi.org/10.1038/nmeth.1517
119. Simão, F. A.; Waterhouse, R. M.; Ioannidis, P.; Kriventseva, E. V.; Zdobnov, E. M. BUSCO: assessing genome assembly and annotation completeness with single-copy orthologs. *Bioinformatics* **2015**, *31*(19), 3210-3212. https://doi.org/10.1093/bioinformatics/btv351

120. Huang, X.; Madan, A. CAP3: A DNA Sequence Assembly Program. *Genome Res.* **1999**, *9*(9), 868–877. https://doi.org/10.1101/gr.9.9.868
121. Gilbert, D. (2013). EvidentialGene Genome Informatics Software May 2013.
122. Altschul, S. F.; Gish, W.; Miller, W.; Myers, E. W.; Lipman, D. J. Basic local alignment search tool. *J. Mol. Biol.* **1990**, *215*(3), 403–410. https://doi.org/10.1016/S0022-2836(05)80360-2
123. Yi, L.; Liu, L.; Melsted, P.; Pachter, L. A direct comparison of genome alignment and transcriptome pseudoalignment. BioRxiv 2018, 444620. https://doi.org/10.1101/444620
124. Robinson, M. D.; McCarthy, D. J.; Smyth, G. K. edgeR: A Bioconductor package for differential expression analysis of digital gene expression data. *Bioinformatics* **2010**, *26*(1), 139–140. https://doi.org/10.1093/bioinformatics/btp616
125. Subramanian, A.; Tamayo, P.; Mootha, V. K.; Mukherjee, S.; Ebert, B. L.; Gillette, M. A.; Paulovich, A.; Pomeroy, S. L.; Golub, T. R.; Lander, E. S.; Mesirov, J. P. Gene set enrichment analysis: A knowledge-based approach for interpreting genome-wide expression profiles. *Proc. Natl. Acad. Sci. U.S.A.* **2005**, *102*(43), 15545–15550. https://doi.org/10.1073/pnas.0506580102
126. Shannon, P.; Markiel, A.; Ozier, O.; Baliga, N. S.; Wang, J. T.; Ramage, D.; Amin, N.; Schwikowski, B.; Ideker, T. Cytoscape: A Software Environment for Integrated Models of Biomolecular Interaction Networks. *Genome Res.* **2003**, *13*(11), 2498–2504. https://doi.org/10.1101/gr.1239303